IOP PUBLISHING BIOINSPIRATION & BIOMIMETICS
Bioinsp. Biomim. **3** (2008) 016001 (10pp) doi:10.1088/1748-3182/3/1/016001

Acoustic pathways revealed: simulated sound transmission and reception in Cuvier's beaked whale (*Ziphius cavirostris*)

Ted W Cranford[1], Petr Krysl[2] and John A Hildebrand[3]

[1] Biology Department, San Diego State University, San Diego, CA 92182, USA
[2] Jacobs School of Engineering, University of California at San Diego, La Jolla, CA 92093, USA
[3] Scripps Institution of Oceanography, University of California San Diego, La Jolla, CA 92093, USA

E-mail: tcranfor@mail.sdsu.edu

Received 30 July 2007
Accepted for publication 19 December 2007
Published 4 February 2008
Online at stacks.iop.org/BB/3/016001

Abstract
The finite element modeling (FEM) space reported here contains the head of a simulated whale based on CT data sets as well as physical measurements of sound-propagation characteristics of actual tissue samples. Simulated sound sources placed inside and outside of an adult male Cuvier's beaked whale (*Ziphius cavirostris*) reveal likely sound propagation pathways into and out of the head. Two separate virtual sound sources that were located at the left and right phonic lips produced beams that converged just outside the head. This result supports the notion that dual sound sources can interfere constructively to form a biologically useful and, in fact, excellent sonar beam in front of the animal. The most intriguing FEM results concern pathways by which sounds reach the ears. The simulations reveal a previously undescribed 'gular pathway' for sound reception in *Ziphius*. Propagated sound pressure waves enter the head from below and between the lower jaws, pass through an opening created by the absence of the medial bony wall of the posterior mandibles, and continue toward the bony ear complexes through the internal mandibular fat bodies. This new pathway has implications for understanding the evolution of underwater hearing in odontocetes. Our model also provides evidence for receive beam directionality, off-axis acoustic shadowing and a plausible mechanism for the long-standing orthodox sound reception pathway in odontocetes. The techniques developed for this study can be used to study acoustic perturbation in a wide variety of marine organisms.

1. Introduction

The cephalic anatomy of toothed whales is marked by structural complexes that have long been recognized as components of a sophisticated biosonar system. This sonar system has three categorical divisions: the sound generation and transmission apparatus, the sound reception and transduction apparatus and the central nervous system components that control output and interpret input. The current paper will present results that touch upon the first two categories.

Several structures within the odontocete head are involved in the production or reception of biosonar sounds (Cranford and Amundin 2003). The nasal apparatus in all odontocetes, as compared to all other mammals, is greatly enlarged, fitted with specialized lipid organs, and a set of skull bones that form an amphitheater-like shape. The melon is composed of fatty tissues; it occupies the amphitheater-like face of the skull

and acts as an acoustic channel and an impedance matching device for sounds propagating out of the head (Cranford and Amundin 2003). Current understanding of the structure and function of the odontocete nasal complex is based on data from a taxonomically diverse handful of species.

The sound generation and transmission apparatus is composed primarily of structures that are nasal in origin. The comparative anatomy of this region has been studied in some detail across the entire odontocete suborder (Norris *et al* 1961, Norris 1964, Schenkkan 1973, Mead 1975, Heyning 1989, Cranford *et al* 1996, Cranford 1999). Only in recent years have we been able to ascertain the site and generation mechanism for sonar signals in bottlenose dolphins (Cranford 2000, Cranford and Amundin 2003). It is unclear whether or not other odontocetes are using homologous structures and similar means but it is at least reasonable based on overall structural similarities (i.e., all odontocetes have a similarly telescoped skull; a fatty melon or its homologue; and two pairs of phonic lips with their associated tissue complexes, except for the special case of the sperm whale). For reviews see Cranford (1992), Cranford *et al* (1996) and Cranford and Amundin (2003).

The sound reception apparatus (sound channels and ears) is located along the ventral aspect of the skull and is associated with the mandibles. With respect to understanding odontocete echolocation, one of the most important questions to answer is: Where does sound enter the head of odontocetes and how does it reach potentially vulnerable structures within the hearing apparatus? This seemingly simple question has not been adequately addressed for any odontocete.

The lower half of the head contains the mandibles, specific masses of acoustic fat associated with sound reception, air-filled pterygoid sinus and the bony ear (tympanoperiotic) complex. There is a long-standing notion that sound enters the odontocete head through a structure known as the 'acoustic window' (Norris 1968), a fat body overlying the posterior portions of the lower jaws, after which it traverses the jaw and enters the internal mandibular fat body on the way to the bony ear complex. This idea, also known as 'jaw hearing', is based primarily upon anatomy (Norris 1964, 1968, 1969) and a group of psychoacoustic experiments exemplified by Brill and Harder (1991), who placed a neoprene hood over the jaws and throat region of a bottlenose dolphin (*Tursiops truncatus*) to exclude sound. They reported a severe degradation in echolocation ability with the application of the hood.

Hearing is the culmination of a set of complex processes. In odontocetes, it involves a directivity index that is frequency dependent and structurally mediated; filtering, focusing and transduction, which are also structurally mediated; and central nervous system processing. Most of what we know about hearing in odontocetes is the result of study and experimentation with a single species, the bottlenose dolphin (*Tursiops truncatus*). Any extrapolation from the results of work with *Tursiops* to other species should be undertaken with trepidation, particularly as one proceeds farther afield taxonomically. At the same time, similar results between disparate species may indicate that a common structure/function paradigm is at work or it may argue for convergent evolution mechanisms.

The pathway of sound to the hearing apparatus (tympanoperiotic complex) is the major thrust of this paper. Our studies indicate that the notion of jaw hearing needs refinement, particularly in light of applicable results from the literature. We will also report preliminary results regarding beam formation for sounds transmitted from the animal, as well as another failed test of the laryngeal phonation hypothesis (see review in Cranford and Amundin (2003)). These additional results also bear upon the process of model validation.

Our FEM studies provide a window into structurally mediated processes, which result from the complex interactions between sounds and anatomy. We can, for the first time, model and simulate acoustic pathways in odontocetes. The majority of prior acoustic research into odontocetes is based upon the end result of complex functions as a whole, rather than isolating various aspects of it. The application of FEM allows us to ask questions that consider systems of structures or their isolated contributions. It also provides a means to manipulate the characteristics of structures or systems of structures and conduct virtual experiments to tease apart the contributions to the overall behavior of the acoustic components. Some of these experiments are underway and will be reported elsewhere.

2. Methods

This study capitalizes on the recent availability of industrial CT scanners to collect data from postmortem whales. Over the past 10 years, one of us (Cranford) has developed and tested a technique to scan large cetacean specimens (Cranford 1999). Once obtained the CT scans can be applied to a wide variety of research questions. Foremost among them is the current effort to advance understanding of the interaction between sound and the anatomy of a whale. We have combined the anatomic geometry obtained from industrial CT scanners, tissue property measurements and custom FEM software ('Vibro-acoustic Toolkit') to produce the 'Vibro-acoustic Simulator' (VAS) (Krysl *et al* 2006, 2007), which simulates sounds and their propagation pathways into and out of the specimens represented by these scans.

The heads of two specimens (one neonate female and one adult male) of *Ziphius cavirostris* were frozen to preserve tissue quality, placed in registration frames, and scanned using X-ray CT. After scanning, the specimens were thawed, photographed and dissected. The use of frozen and thawed tissue in anatomy and acoustic studies was supported by McKenna and her colleagues (McKenna *et al* 2007). The neonate female was CT scanned a second time after being thawed. During dissection the tissues were sampled so that the physical properties (sound velocity and elasticity) could be measured, as reported by Soldevilla and her colleagues Soldevilla *et al* (2005). The elasticity values along with the density information given by the scanning process were incorporated into functional/geometric models of the whales' heads. We were unable to measure the tissue properties in the adult male so the values for the elastic properties in the neonate were also applied to the tissues in the adult male model. The

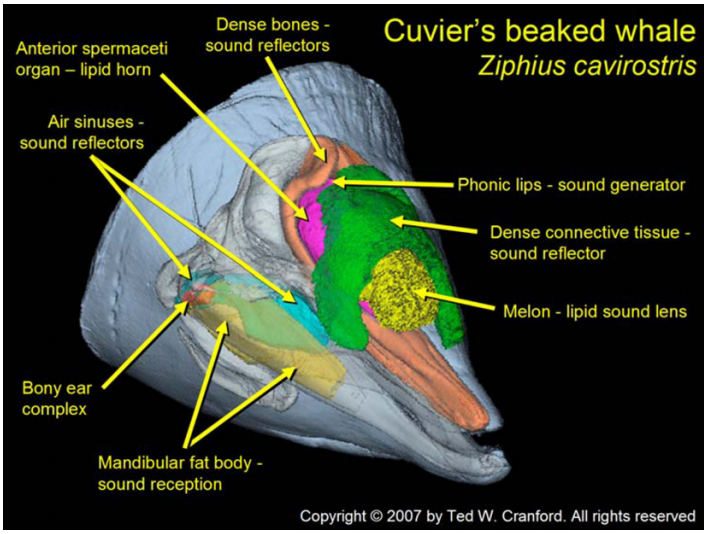

Figure 1. This is a pseudo-3D view of the major components of the biosonar system in *Ziphius cavirostris*. The melon (yellow) is a fat and connective tissue organ that conducts the sound beam out of the head. The sound generation process begins at the phonic lips, located at the posterior extent of the anterior spermaceti organ (magenta), tucked under the overhanging high-density nasal bones forming the prenarial basin (red) of the skull (ivory). Another component of the beam formation apparatus is the dense connective tissue arch (green). The components of the sound reception apparatus are nestled medial to the mandibles: the mandibular fat body (yellow), the pterygoid sinus and the peribullary sinus (cyan), and the bony ear complex (red). The hyoid bones (ivory) hang down below the jaws in the image.

tissue properties can easily be changed in the VAS and we will test the effects of changing them in future work. The results of prior work (Aroyan *et al* 1992) suggest that changing the tissue properties by as much as 10% has little effect on the resultant propagation model but we will investigate this idea further.

We have developed a comprehensive formulation for vibro-acoustic problems in medicine and biology and placed it in the context of a 'toolbox', the vibro-acoustic toolkit. In order to address the difficult problem of discretizing anatomic geometries, the mesh is voxel based, and is generated automatically from common biomedical data sets (CT scans and MRI). The vibro-acoustic toolkit implements a fully Lagrangean finite element formulation based on the decomposition of incident and scattered fields that has been developed to incorporate seamless coupling of fluids and viscoelastic solids, and to allow for accurate representation of incident acoustic excitation (Krysl *et al* 2007).

The propagation of the mechanical (acoustic) disturbance in biological tissues is simulated with the finite element method using the concept of lumping. The inertial effects are accounted for by lumping the distributed mass into point-like particles; the interaction of these particles with each other through the intervening material is accounted for by lumping the elastic and viscous resistance of the material. This produces linkages between the particles through 'springs' reacting to differences in displacement or differences in velocity between the particles.

Our approach is based on the superposition principle and is described in detail elsewhere (Krysl *et al* 2007). The computational model has been verified on common fluid–structure acoustic interaction benchmarks: step-wave interaction with a hollow thin-walled cylinder and scattering from an elastic solid sphere (Krysl *et al* 2007). The displacement field (vector function with three components of displacement along each Cartesian axis) is split into the incident field (known, typically corresponding to a planar or spherical sound wave in the infinite fluid medium in which everything is embedded), and the disturbance (perturbation) field (unknown; it is due to the presence of other fluids or solids, or cavities in the infinite surrounding medium).

The 3D space or 'model space' in which the simulations take place can be imagined as an elongate square column containing the centered head of an adult male *Ziphius cavirostris*, where the remaining space outside the head is filled with sea water. In the model, simulated sound sources can be placed inside of the head or outside of it in the sea water. Most of the simulations used a constant frequency signal at 40 kHz because the echolocation signals recorded from these animals in the wild are narrow-band with a 40 kHz peak frequency (Johnson *et al* 2004, Zimmer *et al* 2005). We also simulated short-duration impulse signals.

3. Results

The first simulations began with sound sources in the head at the phonic lips, known to be the source of sonar signals in the bottlenose dolphin (Cranford and Amundin 2003). The forehead anatomy in *Ziphius cavirostris* (figure 1) and *Tursiops truncatus* is based upon similar basic structural outlines (Cranford 1992, McKenna 2005). If a forwardly

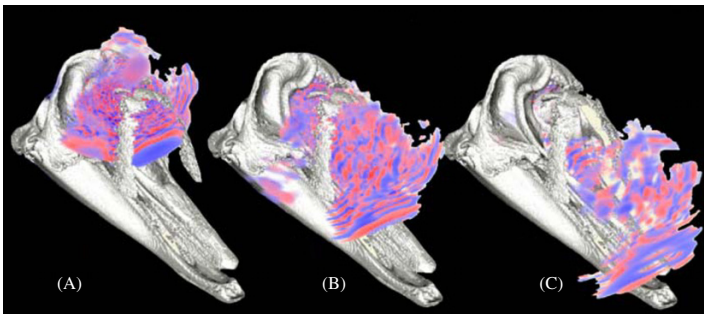

Figure 2. Formation of a forwardly directed sound transmission beam. Three frames from a simulated 40 kHz sound source at the right phonic lips. All of the anatomy was used in the simulation but most of the anatomic structures were made transparent for rendering these frames in order to show the emerging beam. The skull, mandibles and connective tissue arch remain opaque in order to orient the reader. Red indicates positive sound pressure and blue is negative sound pressure.

directed sound beam was generated in the simulations (as has been measured in *Tursiops* and a few other odontocetes) then these first simulations can be seen as a basic validation of the model and methods. The sound beams generated were directed forward and collimated somewhat by the structures along the propagation pathways (figures 1 and 2).

Building, testing and refining the vibro-acoustic simulator (VAS) is an iterative process that relies on validation, and feedback. The results reported here should be seen as emanating from a snapshot in that iterative process.

3.1. Overlapping sound transmission beams

A simulated sound source placed at the phonic lips to the right of the nasal septum (figure 1) produces a beam that emerges from the head after being formed into regular wavefronts (figure 2). A source placed at the complimentary location, the phonic lips to the left of the nasal septum, also produces an acoustic beam with its center axis emerging from the head along the midline. The beams produced from simulated sound sources at the left and right phonic lips overlap in front of the head along the horizontal axis. In our simulations, some of the energy in the forwardly directed beam refracts around the tip of the mandibles, ventrally, and winds up in front of the mouth.

Figure 3 shows that the outgoing signal is different inside the melon than it is just outside the head at the tip of the nose. Note the similarity between the signal at the tip of the nose and one recorded from *Ziphius* in the wild.

3.2. Laryngeal sound source not supported

A significant volume of the early literature contains a debate about whether odontocete biosonar signals, such as most mammal sounds, were generated in the larynx or in the nasal apparatus. Originally, it was assumed that the source of odontocete sonar signals was located in the larynx. The 'laryngeal phonation hypothesis' was put forward largely based on anatomic evidence, sparking a debate that raged in the literature for two decades (reviewed in Cranford (2000) and Cranford and Amundin (2003)). Experimental evidence called this notion into serious doubt beginning in the 1980s (Ridgway *et al* 1980). The bulk of research in the intervening years does not support the laryngeal phonation hypothesis (Cranford and Amundin 2003). We tested the laryngeal phonation hypothesis in *Ziphius* using the VAS and found that a sound source placed at the tip of the larynx does not produce a forwardly directed beam, rendering it improbable as a biosonar source.

3.3. Multiple sound reception pathways

How or by which pathways does sound reach the hearing apparatus? The answers to this question are important for understanding the function of odontocete echolocation as well as potential impacts from exposure to anthropogenic sound.

3.3.1. The 'old' or conventional sound pathway. The conventional sound reception pathway for odontocetes is known by the colloquial term, 'jaw hearing', first put forth by Norris in 1968. A detailed study of mandibular structure led him to propose that sound entered the odontocete head through a fatty pad, the 'acoustic window' (Norris 1968, 1974). This fat pad lies between the skin and the thin posterior portion of each mandible or 'pan bone'. Odontocete mandibles are hollow and the medial bony wall or lamina is absent. These mandibular cavities are filled with pellucid fat bodies. These internal mandibular fat bodies extend posteriorly to form a channel and attachment to the bony ear complexes (tympanoperiotic)[4]. According to Norris, sound passes from the acoustic window through the thin external bony lamina of the pan bone and propagates along the internal mandibular fat body to the tympanoperiotic complexes.

There have been several studies that have attempted to validate or discount Norris' jaw hearing hypothesis (see review in Ketten (2000)) but a mechanism for how sound traverses the pan bones has never been proposed.

We tested the jaw hearing hypothesis with the VAS. These findings indicate that jaw hearing requires a specialized

[4] The fatty channels are ubiquitous to all odontocetes but the chemical composition of those lipids depends upon taxonomy (Koopman *et al* 2006).

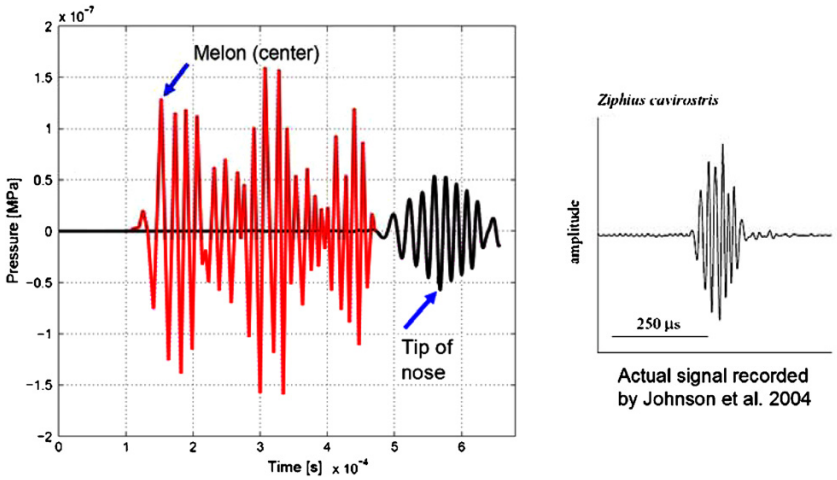

Figure 3. Acoustic signals that are transmitted through the head are apparently shaped by the propagation pathway. In the above case, the initial signal in the simulation began at the phonic lips on the right (Cranford *et al* 2008) and used an initial velocity applied radially to a small volume in the form of a hill function (See Krysl *et al* (2007)). Two virtual receivers recorded the output during the same simulation, one from within the mid portion of the melon and the other just outside of the head near the tip of the rostrum. The dramatic difference between the model signal sampled from within the melon and that at the tip of the nose indicates that significant shaping or conditioning of the signal occurs along the sound propagation pathway. We can also see that the signal at the tip of the nose looks remarkably similar to a signal that was recorded from *Ziphius cavirostris* in the wild (Johnson *et al* 2004) (Reproduced by permission).

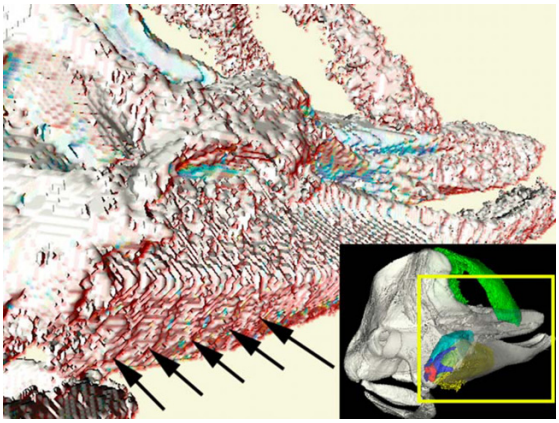

Figure 4. The FEM tools suggest that a flexural wave in the mandibles may explain the mechanism of the 'jaw hearing' theory in odontocetes (Norris 1968). The main part of the figure above is from a simulation where the sound source was 40 kHz, and 0° elevation above the horizontal. The inset image at the lower right shows a context image and a frame that approximates the view seen in the simulation at the left. In the simulation, the flexural wave peaks are indicated by the black arrows and can be seen traveling posteriorly along the jaw. These waves have been exaggerated for the purposes of visualization.

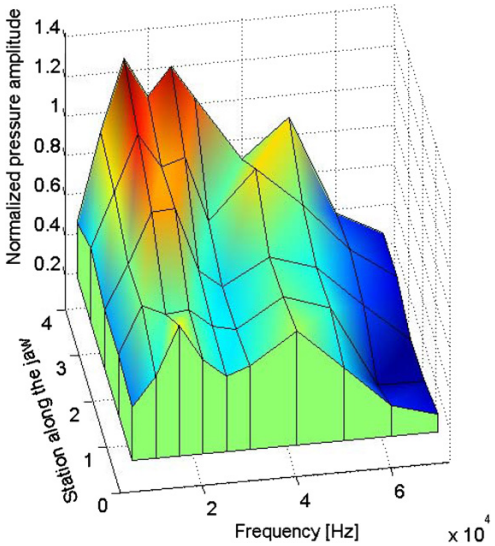

Figure 5. Efficiency of pressure transmission through the mandible as a function of frequency. This graph shows the normalized pressure amplitude along the jaw as a function of frequency. Pressure peaks occur near 20 kHz and 40 kHz at posterior stations of the lower jaw and the efficiency rises posteriorly (stations 0–4).

mechanism to account for sound passing through bone. Simulated sound waves that are incident upon the jaws within specific angles of attack (i.e., from in front of and slightly to one side or the other of the animal) produce a series of small amplitude waves that flex specific regions of the pan bone of the mandible (figure 4). This flexural wave mechanism for jaw hearing is the first explanation for how sound crosses the pan bone.

Figure 5 shows the result of a parametric study that computed the pressure amplitude at various stations along the interior jaw for vibrations transmitted exclusively *through*

the jaw. The parameter is the frequency of the incident planar harmonic acoustic wave. The graph shows the pressure amplitude at a series of stations along the pan bone (anterior to posterior, where station 0 is the point where the mandible becomes single-walled anteriorly, and station 4 is at a point near the temporomandibular joint, where the jaw is joined to the skull). The pressure is normalized by the amplitude of the incident pressure wave at infinity. Note that the amplitude of the pressure wave on the outside of the mandible is typically much higher (about 1.5 to 2 times higher) than the amplitude of the incident pressure wave at infinity. Therefore, the normalized pressure amplitude measured in the interior and equal to 1 means that the mandible is 'transparent' as a measure of how much the mandible limits the transmission of sound pressure between the outside and the inside. Since the amplitude of the pressure acting on the mandible from the outside is typically higher than the amplitude of the incident pressure at infinity, the efficiency may be higher than 1. The presence of the mandible creates a pressure perturbation (essentially boosting the pressure amplitude both on the inside and outside). On the other hand, it also causes reflections which shield the interior from the incident pressure. If these two effects are balanced, the efficiency is 1, and the jawbone may be considered 'transparent'. If the shielding prevails, the measured amplitude on the interior is lower than the incident pressure; otherwise, the effect of the pressure boost is bigger than the shielding and efficiency greater than 1 may result.

Two large peaks occur near 15 and 40 kHz (figure 5) after which the normalized pressure drops off precipitously. These peaks indicate that the mandible becomes increasingly transparent posteriorly.

3.3.2. The 'new' sound pathway. In addition to the conventional notion of jaw hearing, our studies indicate that sound reception may also occur by way of the oral cavity and gular region (figure 6). In this example, a simulated 40 kHz planar pressure (p) wave approaches the animal with an angle of incidence of 0° (i.e., horizontal). When the acoustic pressure wave encounters the cone of soft tissues surrounding the head, it refracts around, largely below, and between the mandibles enters the internal mandibular fat bodies through the opening created by the absence of the medial bony wall of the mandible and propagates caudally to the bony ear complex (figure 6). This acoustic pathway to the ears has not been adequately considered. We will refer to this sound reception pathway through the oral cavity and gular region as the 'gular pathway'.

The intensity of the p waves that reach the bony ear complexes are dependant upon angle of incidence, in both the horizontal and vertical planes. For example, if the sound source is placed outside of the head and slightly to the left of the head on the horizontal, the signal reaches the right ear with some time delay (∼100 μs) and diminution (∼6 fold) in intensity (figure 7).

Alternatively, if the sound source is located along the vertical midline axis and is then raised above or lowered below the horizontal, the intensity of the received signal is diminished equally at both ears (figure 8). Frequency filtering, if it occurs along the new gular pathway, is not immediately obvious and will be the subject of future investigations.

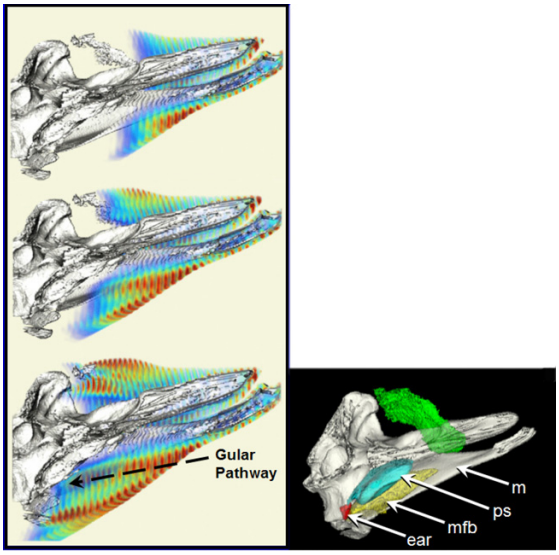

Figure 6. Three frames from an FEM simulation showing the displacement amplitude. In this case, a 40 kHz planar wave was incident upon the specimen from directly in front and 0° above the horizontal. In order to facilitate viewing of the propagation process, the right side of the specimen was removed and only high density structures are displayed during the rendering of the movie frames. But the original simulation included the entire head and all anatomic components. This new 'gular pathway' is shown by waves that refract or wrap around the ventral margin of the mandible, enter the fatty channel on the inside of the mandible and propagate back to the bony ear complex. The inset shows the anatomy that would be found in the simulation frames if it had not been removed to facilitate viewing. The view is of the left side of the head, as viewed from the right. The inset image is reconstructed from CT scans and shows a few important sound reception components, labeled (ear = left tympanoperiotic complex; mfb = left mandibular fat body; ps = left pterygoid sinus; m = left mandible).

4. Discussion

4.1. Sound transmission beams

The mechanism for producing a sound beam is undoubtedly complex and involves contributions from several anatomic components. Figure 3 demonstrates that the signal is 'shaped' or 'conditioned' by the various structures along the propagation pathway. This sort of result can only be discovered by using FEM methods. Fortunately, future studies can take advantage of the flexibility of the simulator, such that the properties of various structures can be changed systematically and the simulation results compared to extract the contributions of the various components.

Of the various components, the pachyosteosclerotic elements of the skull ('Dense bones' colored red in figure 1) apparently play an important roll. There is also a part the sound transmission pathway that includes a large fat body (anterior

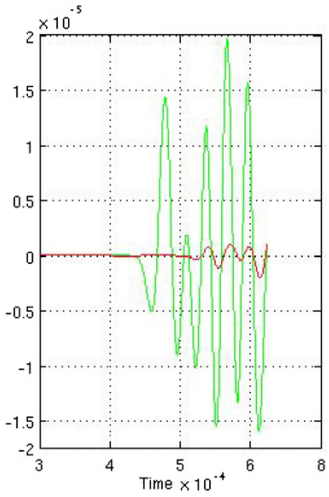

Figure 7. Acoustic shadowing. These records of time versus relative amplitude indicate that there is a time delay and an amplitude diminution in acoustic pressure with respect to each tympanoperiotic complex. In this case the simulated sound source was placed in front of the animal at 0° above the horizontal and less than 2° to the left of the midline. The green trace shows that the acoustic pressure wave arrives earlier in time and at higher amplitude at the left ear than at the right ear. The red trace demonstrates that a collection of anatomic structures shield the right ear complex from sounds that come from sources to the left of the midline.

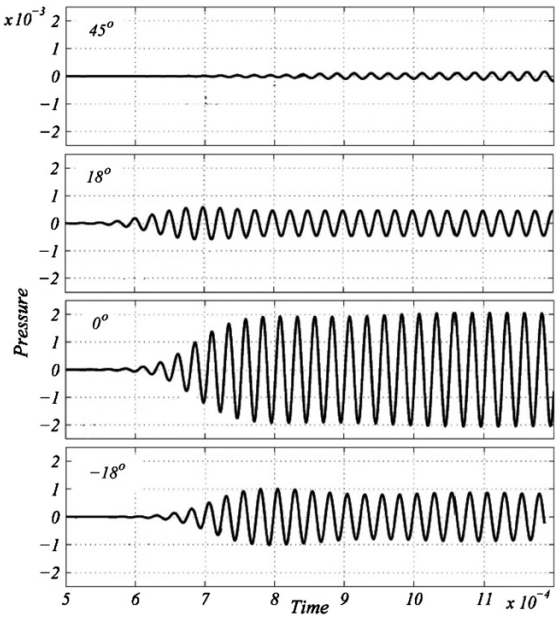

Figure 8. This panel shows that sound pressure amplitude arriving at the left tympanoperiotic complex decreases as the simulated on-axis sound source is moved above or below the horizontal. The lowest intensity arrives from a planar wave that arrives from 45° above the horizontal. The highest intensity arrives from 0° in the vertical plane, i.e., from the horizontal. The abscissa is marked in fractions of a second. The ordinate indicates the relative amplitude.

spermaceti organ) immediately ventral to the melon that is unique to *Ziphius* (figure 1). These anatomic components, and especially the geometry (shapes, sizes and relative interfaces) among the components, are important in the production of a sonar beam (Cranford *et al* 2008).

Readers might be reasonably concerned about the values we have used for tissue elasticity in the model since the gross scale of the samples (Soldevilla *et al* 2005) is not as refined as the scale of the density map given by the CT scans (Cranford *et al* 2008). If there are mistakes in the representation of the tissue properties, it appears that they are relatively small because the simulation results given by figures 2, 3, 7 and 8 are what we should expect considering prior work on a wide variety of odontocetes. Aroyan *et al* (1992) used tissue property values from the literature, gleaned from measurements of various mammalian tissues and produced a simulated transmission beam that approximated those reported in the literature for dolphins. They also reported that changing tissue properties by 5%–10% had little effect on the resultant beam geometry in a CT-based model of *Delphinus delphis*. This notion that the geometry of tissue structures and their interfaces are more important factors in beam formation than any small variation in tissue properties is also supported in our *Ziphius* simulations. For example, in a few probes where we changed the stiffness of the bones up or down by 10% there was no change in the resultant beam shape or direction, but when the stiffness was lower, more energy propagated into the bones. Of course, another possible explanation for answers that approximate reality in a model is that it results from multiple mistakes that cancel one another. This is a possibility that we are always aware of and guard against by constantly checking new results against those from live animal systems.

Independent simulations with sound sources located at the left and right phonic lips produce beams that overlap just outside the head. These results support the notion that sounds generated from two sources (one at each set of phonic lips) may interfere constructively to form a biosonar beam in front of the animal (Cranford and Amundin 2003). This is consistent with current understanding of the biosonar system in the bottlenose dolphin, where left and right phonic lips can operate independently or simultaneously to produce a transmitted sonar beam (Cranford, personal observation).

The simulated beam patterns produced by two sound sources are also consistent with the results obtained by Zimmer and his colleagues (Zimmer *et al* 2005) for free-ranging *Ziphius*. They report that most of the echolocation signals emanate from or near the central axis of the animal's body, normally within 40° of that axis. In our simulations, sound sources placed at either one of the phonic lips locations produced a forwardly directed beam whose axis was near the midline. These results are similar to what has been described for other odontocetes, *Tursiops truncatus* (Au *et al* 1986), *Pseudorca crassidens* (Au *et al* 1995), *Delphinapterus leucas* (Au *et al* 1987) and *Phocoena phocoena* (Au *et al* 1999, 2006), all produce acoustic beams that are similar in shape and direction.

With respect to the beam axis results and the observations of Zimmer and his colleagues, the questions become: Is the

beam axis static in direction with reference to the body axis or can the animal vary the direction of the beam axis? In other words, do these animals have the ability to steer the beam axis, and if so by what means and to what degree?

It is possible that two independent and spatially separated sound sources could be actuated with differing phase relationships to produce a variable beam trajectory or 'beam steering', a function that has also been proposed for non-physeterid odontocetes (Cranford and Amundin 2003). Sonar beam steering has been suggested in harbor porpoises (Amundin 1991) and it has long been suspected for other odontocetes but this question awaits focused investigation. The notion that odontocetes can change the acoustic beam geometry has been measured in the sperm whale (Møhl *et al* 2000). Currently we cannot simultaneously activate two sources within the model space to test the idea of beam steering by phase shifting the sources and interference but are adding these tools to the vibro-acoustic toolkit so that we can address these questions in future studies.

Collectively, the characteristics in the simulated transmission beam and the close approximation to results from studies with live free-ranging animals (Zimmer *et al* 2005) suggests that the collective results from our work with the VAS passes a basic test of validation for the adult male *Ziphius*.

4.2. Sound reception pathways

The gular sound pathway into the ears described herein is a discovery that now seems somewhat conspicuous considering that it provides a virtually an unobstructed path to the hearing apparatus. Norris and Harvey (1974) anticipated that some sound reception might occur through the mouth and throat, particularly when the animal closes in on a target. They did not, however, suspect that the gular pathway might be the primary pathway for sound reception.

There are a couple of 'odd' or isolated lines of evidence in the literature that suggest the gular pathway is functional in the bottlenose dolphin. Møhl and his colleagues Møhl *et al* (1999) reported that the *most* sensitive region for sound entering the head was slightly forward of Norris' acoustic window. Curiously, they also noted a region of high (acoustic) sensitivity along the ventral midline in a bottlenose dolphin (essentially as high as the greatest sensitivity measured), but they did not otherwise comment on this interesting result. We surmise that this unique result for *Tursiops* supports our preliminary results for *Ziphius*, implying broad taxonomic distribution.

If the gular pathway is valid it could only function in the absence of the medial bony lamina of the posterior portion of the mandible, a condition that exists in all toothed whales and their ancestral archaeocetes. Since the medial bony wall is absent in all known odontocetes, we speculate that this gular pathway is functional across the suborder. At the same time, the outer walls of the posterior mandibles in archaeocetes are relatively thick, unlike extant odontocetes, so it may be that the flexural wave mechanism was not functional in the ancient whales. Perhaps the primordial underwater hearing pathway in whales was through the gular region and that jaw hearing was a more recent development.

A technical report (Brill *et al* 2001) found high sensitivity when their 'jawphone' (composed of a suction cup coupled to a hydrophone) was placed slightly anterior to the acoustic window. Unfortunately, they had difficulty maintaining the suction cup attachment of the jawphone at a location on the ventral (gular) side of the head. The work by Brill, Møhl and their colleagues (Brill and Harder 1991, Møhl *et al* 1999, Brill *et al* 2001) clearly supports the jaw hearing hypothesis of Norris (1968) but the mechanism for the transmission of sound across the bony wall of the mandible remains unresolved.

Our FEM simulations suggest that the thinned posterior walls of the lower jaws are forced into a series of flexural waves by incoming sounds, provided that the sounds and bone have a specific set of characteristics. This is one possible explanation for the mechanism of jaw hearing but it is complex and by no means certain. As it turns out, the theoretical basis of this idea had apparently already occurred to Møhl and his colleagues Møhl *et al* (1999). Considering our findings, the comments they made in the last paragraph of their discussion seem prescient:

> 'When evaluating the models, it should be borne in mind that the cross section of the mandible is on the same order of magnitude as the dominant wavelength of *p*-waves (compressional or longitudinal waves, as opposed to transversal and shear waves) in water and soft tissues at 50 kHz (3 cm). A logical consequence of this observation is that models inspired from optical analogies (reflections, refraction, etc) are problematic, as they require structures that are considerably larger than the wavelength. However, in mixed media with solid components, other sorts of waves than compressional, longitudinal ones can be realized'. (Møhl *et al* 1999, p 3424)

Their proposition that combinations of wave types are likely to be operational in mixed media containing solid components, is directly in line with what we see in the VAS simulations. The new gular pathway certainly does not negate Norris' jaw hearing pathway but it does change our understanding of it. One explanation of the flexural wave notion is that pressure (P) waves incident upon the mandibles are translated into P waves and shear (S) waves in the thin posterior bony shell, the pan bone, of the mandible or lower jaw. That this combination (P&S) wave may be in phase with the wave incident upon the mandible to form flexural waves within the thinned pan bone is supported by our simulation results and the assertions of Møhl *et al* (1999). Once the P waves and S waves create flexing in the thin bony wall the sound will propagate into the internal mandibular fat bodies and through them to the bony ear complexes.

The flexural wave mechanism is admittedly complex and there is much work ahead to test the veracity of this proposal. This mandibular mechanism depends upon a number of factors including the geometry and elastic properties of the mandibles and adjacent soft tissues as well as the acoustic frequency and its angle of incidence. There is an indication that the flexing is accentuated by interference between successive pressure

wavefronts reflected from the bones, such that the waves gain amplitude as they travel caudally, resulting in areas along the jaw bone where the pressure is greater than the pressure of the incident planar wave before it reaches the rostrum (figure 5).

Figures 4 and 5 support the flexural wave notion of sound transmission across the mandibles and buttress the case for Norris' acoustic window. Since transmission by this mechanism depends on the elastic properties of the bone, those properties should be measured explicitly for odontocete mandibles. The flexural wave mechanism requires us to sort out a complex set of intermingled physical parameters, a process that is already underway.

One question that arises from the flexural wave proposal involves the possibility that sound transmission through the mandible functions as a kind of 'tonotopic' frequency filter, allowing selected frequencies to pass at certain locations and blocking others. Is there a comparative or discriminative value between sounds arriving via the two pathways (i.e., jaw hearing and gular pathways)? We can conceive that the flexural wave mechanism could cause filtering to occur by preferentially passing frequencies according to the thickness of the bony wall and various other properties of the bone. Norris (1968) has shown that 'C' shaped cross sections of the mandible change gradually in thickness along its length and may therefore pass certain frequencies (e.g., filtering) according to the parameters of mandibular structure and the acoustic signal incident upon it.

In 1984, Au and Moore published the received beam patterns for two bottlenose dolphins using psychoacoustic methods (Au and Moore 1984). The pattern they reported is similar to that shown in figure 8, where the highest sound pressure amplitude received at the ears arrives from directly forward of the rostrum and the received amplitude drops off above and below the horizontal plane. The congruity between the Au and Moore results and our simulations suggest a similar pathway in representatives from vastly different taxa. It is somewhat counterintuitive that a planar sound wave arriving from below horizontal (-18° in figure 8) reaches the ear with a lower amplitude than one arriving from the horizontal. It seems reasonable that sounds originating from below the horizontal axis should have direct and unfettered access to the gular pathway, yet our results and those of Au and Moore (1984) suggest that this is not the case. This evidence suggests that the gular pathway may have a receive beam directivity index and that the mechanism might be generalizable to all odontocetes. Our toolkit should allow us to tease apart the anatomic basis of this mechanism.

The VAS can also use to predict changes to acoustic waveforms at any point in the simulation space as a result of the complex interactions among other structures within the head. Our simulations allow us to predict the time delay and the difference in amplitude between signals that reach the ear complexes from a sound originating in front of the head and off-axis laterally (figure 6). These interaural differences are apparently due in large part to shielding by a suite of anatomic structures. Specifically the juxtaposition of the large pterygoid sinuses, a fibrous venous plexus and lipid-rich pathways that connect the acoustic environment to the bony ear complex provide a means for understanding and delineating the specific contributors to interaural differences. It may be that the time delay, phase differences, or amplitude differences between the gular pathway and jaw hearing pathway provide additional acoustic cues to the animal during biosonar. We will address these questions in future investigations.

These results demonstrate a powerful combination of techniques that provide a reliable, low-cost tool that can be used to investigate questions that probe the interaction between anatomic structure and a limitless choice of sound sources. The value of this technological innovation increases with the taxonomic expansion of the digital library of cetacean anatomy. Finite element modeling facilitates investigations of acoustic exposure across a broad spectrum of species, including non-mammalian aquatic vertebrates.

5. Conclusions

The vibro-acoustic simulations presented here suggest a new acoustic pathway to the ears from around and under the mandibles and that a flexural wave offers a plausible explanation for the conventional pathway through the thinned mandibles as originally described by Norris (1968, 1974).

The fact that a source placed at either of the phonic lip locations produces a narrow, forwardly directed beam leads to plausible functional explanations. These sound transmission simulations also support the notion that if sounds are generated at both (left and right) phonic lips at the same (or nearly the same) time, they could converge into a beam with higher amplitude than might be produced by either source independently due to constructive interference. This is the kind of information that has never been verified for other odontocetes, even though a few workers have suspected that this is the case. When we move to simulations of other odontocetes we will be able to test whether it holds true and suggests a concept that is broadly applicable.

The gular pathway for sound propagation in odontocetes creates a new vision and significant implications for our understanding of hearing and a means for evaluating the potential impacts of high-intensity sound. It is clear from these results that the acoustic structure and function of the odontocete head deserve considerable additional research.

Finally, the results reported here must be considered with a healthy dose of skepticism because the simulations push beyond our current knowledge base for this species. At the same time, we have provided examples suggesting that the FEM-based method produces results that are reasonable and may substantially improved our understanding of odontocete bioacoustics.

Acknowledgments

This research was supported by Chief of Naval Operations (CNO 45). Special thanks are due to Frank Stone and Ernie Young (CNO 45) and Professor Curtis A Collins, Department of Oceanography at the Naval Postgraduate School, Monterey, California. The success of this research is also due in part to previous support of the senior author by Dr Robert Gisiner at

the Office of Naval Research. This paper has benefited from reviews by Carl Schilt and three anonymous reviewers.

References

Amundin M 1991 *Sound Production in odontocetes with emphasis on the harbour porpoise Phocoena phocoena* (Stockholm, Sweden: Department of Zoology, University of Stockholm) p 128

Aroyan J L, Cranford T W, Kent J and Norris K S 1992 Computer modeling of acoustic beam formation in *Delphinus delphis J Acoust. Soc. Am.* **92** 2539–45

Au W W L, Kastelein R A, Benoit-Bird K J, Cranford T W and McKenna M F 2006 Acoustic radiation from the head of echolocating harbor porpoises (*Phocoena phocoena*) *J. Exp. Biol.* **209** 2726–33

Au W W L, Kastelein R A, Rippe T and Schooneman N M 1999 Transmission beam pattern and echolocation signals of a harbor porpoise (*Phocoena phocoena*) *J. Acoust. Soc. Am.* **106** 3699–705

Au W W L and Moore P W B 1984 Receiving beam patterns and directivity indices of the Atlantic bottlenose dolphin *Tursiops truncatus J. Acoust. Soc. Am.* **75** 255–62

Au W W L, Moore P W B and Pawloski D A 1986 Echolocation transmitting beam of the Atlantic bottlenose dolphin *J. Acoust. Soc. Am.* **80** 688–91

Au W W L, Pawloski J L, Nachtigall P E, Blonz M and Gisiner R C 1995 Echolocation signals and transmission beam pattern of a false killer whale (*Pseudorca crassidens*) *J. Acoust. Soc. Am.* **98** 51–9

Au W W L, Penner R H and Turl C W 1987 Propagation of beluga echolocation signals *J. Acoust. Soc. Am.* **82** 807–13

Brill R L and Harder P J 1991 The effects of attenuating returning echolocation signals at the lower jaw of a dolphin (*Tursiops truncatus*) *J. Acoust. Soc. Am.* **89** 2851–7

Brill R L, Moore P W B, Helweg D A and Dankiewicz L A 2001 *Investigating the Dolphin's Peripheral Hearing System: Acoustic Sensitivity about the Head and Lower Jaw* (San Diego, CA: SPAWAR Systems Center) p 20

Cranford T W 1992 *Functional Morphology of the Odontocete Forehead: Implications for Sound Generation* (California: Department of Biology, University of California Santa Cruz) p 276

Cranford T W 1999 The sperm whale's nose: Sexual selection on a grand scale? *Mar. Mamm. Sci.* **15** 1134–58

Cranford T W 2000 In search of impulse sound sources in odontocetes *Hearing by Whales and Dolphins* ed W W L Au, A N Popper and R R Fay (New York: Springer) pp 109–56

Cranford T W and Amundin M E 2003 Biosonar pulse production in odontocetes: the state of our knowledge *Echolocation in Bats and Dolphins* ed J A Thomas, C F Moss and M Vater (Chicago, IL: University of Chicago Press) pp 27–35

Cranford T W, Amundin M and Norris K S 1996 Functional morphology and homology in the odontocete nasal complex: implications for sound generation *J. Morphol.* **228** 223–85

Cranford T W, McKenna M F, Soldevilla M S, Wiggins S M, Goldbogen J A, Shadwick R E, Krysl P, St Leger J A and Hildebrand J A 2008 Anatomic geometry of sound transmission and reception in Cuvier's beaked whale (*Ziphius cavirostris*) *Anat. Record* **291** online, doi 10.1002/ar.20652

Heyning J E 1989 Comparative facial anatomy of beaked whales (*Ziphiidae*) and a systematic revision among the families of extant Odontoceti *Contr. Sci. Los Angeles County Mus.* **405** 1–64

Johnson M, Madsen P T, Zimmer W M X, Aguilar de Soto N and Tyack P L 2004 Beaked whales echolocate on prey *Proc. R. Soc. Lond.* B (suppl.) **271** S383–6

Ketten D R 2000 Cetacean ears *Hearing by Whales and Dolphins* ed W W L Au, A N Popper and R R Fay (New York: Springer) pp 43–108

Krysl P, Cranford T W and Hildebrand J A 2007 Lagrangian finite element treatment of transient vibration/acoustics of biosolids immersed in fluids *Int. J. Numer. Methods Eng.* online, doi 10.1002/nme.2192

Krysl P, Cranford T W, Wiggins S M and Hildebrand J A 2006 Simulating the effect of high-intensity sound on cetaceans: modeling approach and a case study for Cuvier's Beaked whale (*Ziphius cavirostris*) *J. Acoust. Soc. Am.* **120** 2328–39

McKenna M F 2005 *Comparative Morphology of the Odontocete Melon: Functional and Evolutionary Interpretations* San Diego Biology Department, San Diego State University p 197

McKenna M F, Goldbogen J A, St. Leger J A, Hildebrand J A and Cranford T W 2007 Evaluation of postmortem changes in tissue structure in the bottlenose dolphin (*Tursiops truncatus*) *Anat. Rec.* **290** 1023–32

Mead J G 1975 Anatomy of the external nasal passages and facial complex in the Delphinidae (Mammalia: Cetacea) *Smithson. Contrib. Zool.* **207** 1–72

Møhl B, Au W W L, Pawloski J and Nachtigall P E 1999 Dolphin hearing: relative sensitivity as a function of point of application of a contact sound source in the jaw and head region *J. Acoust. Soc. Am.* **105** 3421–4

Møhl B, Wahlberg M, Madsen P T, Miller L A and A S 2000 Sperm whale clicks: directionality and Source level revisited *J. Acoust. Soc. Am.* **107** 638–48

Norris K S 1964 Some problems of echolocation in cetaceans *Marine Bio-acoustics* ed W N Tavolga (New York: Pergamon) pp 317–36

Norris K S 1968 The evolution of acoustic mechanisms in odontocete cetaceans *Evolution and Environment* ed E T Drake (New Haven: Yale University Press) pp 297–324

Norris K S 1969 The echolocation of marine mammals *The Biology of Marine Mammals* ed H T Andersen (New York: Academic) pp 391–423

Norris K S 1974 *The Porpoise Watcher* (New York: W W Norton)

Norris K S and Harvey G W 1974 Sound transmission in the porpoise head *J. Acoust. Soc. Am.* **56** 659–64

Norris K S, Prescott J H, Asa-Dorian P V and Perkins P 1961 An experimental demonstration of echolocation behavior in the porpoise, *Tursiops truncatus* (Montagu) *Biol. Bull.* **120** 163–76

Ridgway S H, Carder D A, Green R F, Gaunt A S, Gaunt S L L and Evans W E 1980 Electromyographic and pressure events in the nasolaryngeal system of dolphins during sound production *Animal Sonar Systems* ed R G Busnel and J F Fish (New York: Plenum) pp 239–50

Schenkkan E J 1973 On the comparative anatomy and function of the nasal tract in odontocetes (Mammalia, Cetacea) *Bijdr Dierk* **43** 127–59

Soldevilla M S, McKenna M F, Wiggins S M, Shadwick R E, Cranford T W and Hildebrand J A 2005 Cuvier's beaked whale (*Ziphius cavirostris*) head tissues: physical properties and CT imaging *J. Exp. Biol.* **208** 2319–32

Zimmer W M X, Johnson M P, Madsen P T and Tyack P L 2005 Echolocation clicks of free-ranging Cuvier's beaked whales (*Ziphius cavirostris*) *J. Acoust. Soc. Am.* **117** 3919–27

The Journal of Experimental Biology 212, 3100-3107
Published by The Company of Biologists 2009
doi:10.1242/jeb.030825

Acoustic behaviour of echolocating porpoises during prey capture

Stacy L. DeRuiter[1,2,*], Alexander Bahr[3], Marie-Anne Blanchet[4], Sabina Fobian Hansen[5], Jakob Højer Kristensen[5], Peter T. Madsen[6,2], Peter L. Tyack[2] and Magnus Wahlberg[5,7]

[1]IFREMER, Service Acoustique et Sismique, B.P. 70, 29280 Plouzané, France, [2]Biology Department, Woods Hole Oceanographic Institution, Woods Hole, MA 02543, USA, [3]Massachusetts Institute of Technology, Center for Ocean Engineering, 32 Vassar Street, Cambridge, MA 02139, USA, [4]Idrettsvein 40B, 9009 Tromsø, Norway, [5]Fjord and Baelt, Margrethes Plads 1, DK-5300 Kerteminde, Denmark, [6]Department of Biological Sciences, Zoophysiology, Aarhus University, C.F. Møllers Allé, Building 1131, DK-8000 Aarhus C, Denmark and [7]Marine Biological Laboratory, University of Southern Denmark, Hindsholmsvej 10, 5300 Kerteminde, Denmark

*Author for correspondence (stacy_deruiter@yahoo.com)

Accepted 30 June 2009

SUMMARY

Porpoise echolocation has been studied previously, mainly in target detection experiments using stationed animals and steel sphere targets, but little is known about the acoustic behaviour of free-swimming porpoises echolocating for prey. Here, we used small onboard sound and orientation recording tags to study the echolocation behaviour of free-swimming trained porpoises as they caught dead, freely drifting fish. We analysed porpoise echolocation behaviour leading up to and following prey capture events, including variability in echolocation in response to vision restriction, prey species, and individual porpoise tested. The porpoises produced echolocation clicks as they searched for the fish, followed by fast-repetition-rate clicks (echolocation buzzes) when acquiring prey. During buzzes, which usually began when porpoises were about 1–2 body lengths from prey, tag-recorded click levels decreased by about 10 dB, click rates increased to over 300 clicks per second, and variability in body orientation (roll) increased. Buzzes generally continued beyond the first contact with the fish, and often extended until or after the end of prey handling. This unexplained continuation of buzzes after prey capture raises questions about the function of buzzes, suggesting that in addition to providing detailed information on target location during the capture, they may serve additional purposes such as the relocation of potentially escaping prey. We conclude that porpoises display the same overall acoustic prey capture behaviour seen in larger toothed whales in the wild, albeit at a faster pace, clicking slowly during search and approach phases and buzzing during prey capture.

Key words: echolocation, porpoise, foraging, buzz, biosonar, *Phocoena*.

INTRODUCTION

Echolocating animals can gather information about their environment by emitting sound pulses, then processing echoes returning from ensonified objects in the environment. Echolocation, or biosonar, is used to aid orientation during navigation and foraging, and has been found in various taxa including bats, whales and cave-dwelling birds (Griffin, 1958; Thomas et al., 2004). Detailed studies of the echolocation strategies of various species can provide insight into their foraging ecology and uncover specific features that adapt echolocation to particular niches.

Echolocation by most foraging bats consists of several distinct phases: first, a search phase consisting of regularly spaced echolocation signals; next, an approach phase, in which the bat focuses its attention on one prey target, often with an increasing repetition rate as the bat begins to approach the prey; then, a terminal phase, during which echolocation signals are emitted at an even faster, increasing repetition rate (Schnitzler and Kalko, 2001; Thomas et al., 2004). Often, each phase of echolocation is characterized by specific signal waveforms and patterns of signal repetition rate (Schnitzler and Kalko, 2001). The terminal phase is also termed the buzz (Griffin, 1958); in this phase acoustic characteristics of the echolocation clicks are specialised for precise target localization and range determination, and the more closely spaced clicks provide more frequent updates of prey location (Britton and Jones, 1999). Bat buzz production generally stops at the time of prey capture or slightly before; after a buzz, bats generally pause echolocation click production for a period of tens to hundreds of milliseconds (Britton and Jones, 1999; Griffin et al., 1960; Hartley, 1992; Hiryu et al., 2007; Kalko, 1995; Kalko and Schnitzler, 1989; Moss and Surlykke, 2001).

A few species of toothed whales have been shown experimentally to use echolocation for navigation or for prey detection and capture, and all other toothed whales recorded to date produce clicks with source properties and signal repetition rates suitable for echolocation, so they are all thought to employ biosonar (Au, 1993; Evans, 1973; Møhl et al., 2003; Reynolds and Rommel, 1999). A sequence of acoustic events analogous to that described for bats has been recorded from echolocating harbour porpoises *Phocoena phocoena* (Verfuss et al., 2009), narwhals *Monodon monoceros* (Miller et al., 1995), sperm whales *Physeter macrocephalus* (Madsen et al., 2002b; Miller et al., 2004), and beaked whales *Mesoplodon densirostris* and *Ziphius cavirostris* (Johnson et al., 2008; Johnson et al., 2004; Madsen et al., 2005). Thus, all toothed whale species studied emit regularly spaced clicks, thought to be functionally analogous to the search phase of bat echolocation, and they also produce buzzes, as bats do (Johnson et al., 2004; Madsen et al., 2002b; Miller et al., 1995; Miller et al., 2004; Thomas et al., 2004). Click rate is not the only feature distinguishing buzzes from regular echolocation clicks; both sperm whale and beaked whale buzz clicks have intensities about 20 dB below the average regular click intensity (Madsen et al., 2005; Madsen et al., 2002b), and the buzz clicks of Blainville's beaked whales are distinguishable from frequency-

modulated search clicks by their shorter duration, higher frequency and lack of frequency modulation (Johnson et al., 2006). Buzz production rate has been proposed as a proxy for toothed whale foraging success rate (Madsen et al., 2002b; Miller et al., 2004; Watwood et al., 2006).

Aside from the statement that trained harbour porpoises end their buzzes 'shortly after the catch' (Verfuss et al., 2009), published data on toothed whales do not indicate whether prey capture occurs during or after the buzz. For beaked whales and sperm whales, capture has been assumed to occur near the end of the buzz, based on two lines of evidence: the timing of impact sounds in tag audio recordings (Johnson et al., 2004) and the observed increase in dynamic acceleration and body movements during buzzes, thought to indicate sudden movement or manoeuvring related to a capture attempt (Johnson et al., 2004; Miller et al., 2004).

Thus, toothed whales, like many bats, use echolocation. Although the echolocation signal characteristics and target detection abilities of various toothed whale species have been investigated, there have been relatively few experiments that recorded the acoustic behaviour of free swimming animals as they use echolocation to find prey. Tagging studies in the field and work on trained animals have provided data on sound production and animal movements during foraging behaviour for a variety of species, including sperm whales (Madsen et al., 2002a; Miller et al., 2004; Teloni et al., 2008), beaked whales (Johnson et al., 2006; Madsen et al., 2005; Tyack et al., 2006), pilot whales *Globicephala macrorhynchus* (Aguilar Soto et al., 2008), finless porpoises *Neophocaena phocaenoides* (Akamatsu et al., 2005) and harbour porpoises (Akamatsu et al., 2007; Verfuss et al., 2009). While these studies have provided a wealth of information on echolocation click production rates and characteristics in relation to animal depth and movements, only Verfuss and colleagues were able to collect data on timing of capture or prey capture success rates. Their analysis focused specifically on defining the phases of porpoise echolocation and quantifying regular click rate as a function of range to prey (Verfuss et al., 2009).

Several other papers describe and discuss intriguing evidence of variability in the echolocation strategies of beaked whales (Johnson et al., 2008; Madsen et al., 2005) and sperm whales (Teloni et al., 2008). The studies link different prey capture strategies to variation in prey type pursued, as evidenced by variation in whale movement patterns, buzz characteristics, and prey echo characteristics (Johnson et al., 2008) or capture depth (Teloni et al., 2008). However, none of these studies had the means to collect field data on prey species captured other than echo characteristics. Without such data, it is difficult to interpret variability in echolocation strategies in response to the variable backscattering properties of different prey types, and it is not possible to assess how the timing of echolocation phases relates to the actual capture time.

In the current study, we applied archival tags to trained harbour porpoises (*Phocoena phocoena* Linnaeus 1758) as they captured sinking dead fish. The tags logged acoustic and movement data during the prey captures, allowing us to quantify and analyse the animals' detailed echolocation behaviour leading up to and following prey capture events. In contrast to many previous studies, we were able to analyse echolocation click sequences with respect to the timing of prey capture, and we focused on adjustment of click rate and level over the course of a capture and the detailed timing of the buzz. We addressed hypotheses formulated in light of previous toothed whale tagging studies; specifically, that porpoises: (1) initiate echolocation buzzes just before the time of prey capture, when they are about one body length away from the prey fish; (2) terminate those buzzes at the time of prey capture; (3) reduce their click amplitude significantly during buzzes; and (4) respond to differences in experimental conditions (primarily, availability of visual cues and prey type) by varying the timing of their approach to prey and the level and timing of their echolocation clicks.

MATERIALS AND METHODS

Tag development and tag specifications

To carry out the prey capture experiments, a modified version of the Dtag (Johnson and Tyack, 2003) was developed specifically for use with trained harbour porpoises. The porpoise tag records sound data in stereo with a peak clip level of 191 dB re. 1 μPa, digitizing the data at sampling frequencies of up to 500 kHz per channel (16-bit resolution) and storing it in onboard solid state flash memory. Along with sound, the tag synchronously records data from movement sensors (sampled at 50 Hz), including three-axis accelerometers and magnetometers and a pressure sensor, which allow calculation of the animal's acceleration, pitch, roll, heading and depth (Johnson and Tyack, 2003). With lossless data compression, the tag can record about an hour of sound and sensor data in its 3 GB memory. The tag attaches noninvasively, with custom-made suction cups (Fig. 1).

Prey capture experiments

Prey capture experiments took place at Fjord & Baelt in Kerteminde, Denmark, which houses four harbour porpoises. Two porpoises participated in the experiments: Eigil [male; at Fjord & Baelt since April 1997; estimated to be 1- to 2-years old at arrival (Lockyer, 2003)] and Sif [female; at Fjord & Baelt since July 2004; estimated to be about 1-year old at arrival (Lockyer, 2003)]. The animals are housed in a 30×10 m outdoor facility, connected to the harbour by a series of nets, and with a natural sandy and rocky bottom 2–4 m deep. The porpoises were trained to carry the tag using operant conditioning and positive reinforcement (Ramirez, 1999). Addition of the tag did not cause any noticeable alteration in the previously learned prey capture behaviour. The tag was attached dorsally with suction cups, just behind the blowhole, as shown in Fig. 1. At the start of each prey capture trial, a trainer called the tagged porpoise to a station at one end of the experimental pen. On a cue from the trainer, the tagged porpoise was sent across the pen; at the same cue, an assistant at the other end of the pen slapped the water surface with a stick (as an initial orientation cue for the porpoise) and then dropped a fish into the water at the same location. The porpoises' task was to find and eat the fish, then return to the trainer. During each trial, in addition to tag data, we collected underwater video recordings and stopwatch data on the times of key events [trainer cues, fish release, and prey capture (defined as first physical contact between the porpoise's mouth and the fish)]. The tag, video and stopwatch data were all synchronized by simultaneously recording a signal (a short series of gentle taps on the tag housing) on all three records at the start and end of each session. Maximum synchronization error was 0.04 s, since the minimum video capture rate was 25 frames per second.

Trials were conducted with and without eyecups (suction cups that covered the porpoises' eyes like blindfolds and forced them to locate the fish without the aid of vision). We ran 71 prey capture trials between January 9 and January 13, 2008. They were carried out in 12 sessions of four to eight trials per session; all sessions contained trials with and without eyecups and trials with different fish types, as detailed elsewhere (DeRuiter, 2008). Fish used in the trials were dead, frozen then thawed from the same stock that constituted the porpoises' normal diet at Fjord & Baelt. They included herring (*Clupea harengus*, 28 trials, mean fork length

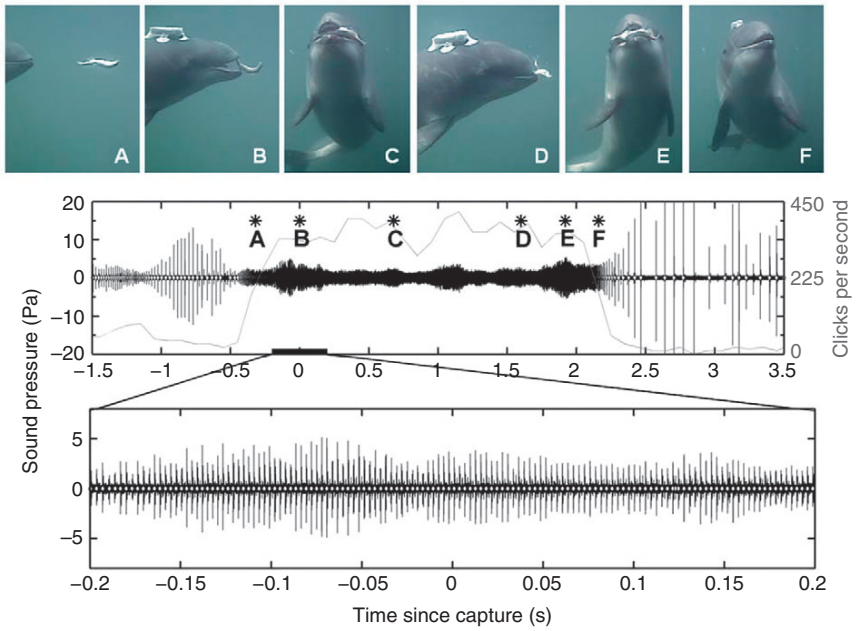

Fig. 1. Images (from underwater video footage) and waveforms (from tag audio recording) during a prey capture event. Time 0 (B) is defined as the moment of prey capture. Asterisks on the upper waveform plot indicate the times at which the photos were taken. The *y*-axis scales are set for optimal viewing of the echolocation buzz (clicks are not clipped in the recording). Clicks detected by the click detector are indicated on the waveform plots as white diamonds at amplitude zero (they are not visible during the buzz in the middle panel because they are too closely spaced in time). The lower waveform is an expanded view of the time of capture to illustrate click level and signal-to-noise ratio during the buzz. In the middle panel, the grey line plots click rate in clicks per second (scale on right *y*-axis).

21.0 cm), capelin (*Mallotus villosus*, 37 trials, mean fork length 15.1 cm), and sprat (*Sprattus sprattus*, six trials, mean fork length 12.6 cm).

Data analysis

For each trial, we used stopwatch data to calculate the time it took the porpoises to catch each fish, defined as the time from the trainer sending the cue until the fish (or part of the fish) was in the porpoise's mouth. Comparison with video data confirmed the accuracy of the stopwatch-measured capture times (stopwatch error had a mean of +0.012 s, and a median absolute value of 0 s, for 40 trials with clear video of the time of capture). Porpoises were never observed to lose fish after having them in their mouths, although they did sometimes manipulate or carry the fish before swallowing them. We applied a two-sample *t*-test to test whether the mean capture duration was different for trials with and without eyecups.

For each trial, a 30-s segment of the tag audio recording was analyzed: 15 s before and 15 s after the stopwatch time of prey capture. Tag audio data were filtered in Matlab (The Mathworks, Natick, MA, USA) with an eight-pole Butterworth bandpass filter between 100 and 200 kHz. Porpoise clicks were detected in the filtered audio recordings using a custom-written envelope-based click detector in Matlab. The click detection algorithm was designed to detect clicks despite high variability in click levels and inter-click intervals in the tag data, as described in detail elsewhere (DeRuiter, 2008). Briefly, the algorithm worked as follows. (1) Calculate the envelope of the audio signal; detect candidate clicks according to an envelope-level detection threshold. (2) After a candidate click is detected, do not detect any additional clicks within 1.3 ms following the initial detection. (This blanking time was selected after manual inspection of prey capture buzzes in the dataset, none of which contained inter-click intervals of less than 1.3 ms.) (3) Compare the maximum envelope level (MEL) of the detected click to L, the mean of the maximum envelope levels of the preceding three clicks. Compare the inter-click interval (ICI) preceding the detected click to I, the mean ICI of the preceding three clicks. Accept the click if MEL≥0.5L and ICI≥0.2I. Also accept clicks for which ICI<0.2I but MEL≥3L. These criteria help reduce detections of surface and bottom reflections. (4) Accept clicks for which MEL<0.5L but ICI>3I. In this case, reset I to 100 ms. This rule allows detection of trains of low amplitude clicks after long inter-click intervals or sudden drops in click level, without promoting detection of quiet reflections and/or echoes between higher amplitude clicks. Click detector performance was checked visually by examining plots of the data waveforms overlaid with click detections. The time (in seconds until prey capture) and received peak-to-peak (pp) level of each detected click was recorded. Animal movement data (specifically roll angle) were filtered and resampled to obtain an effective sampling rate of 5 Hz.

For acoustic time-series analysis, click rate data were binned into 0.1 s bins. To calculate echolocation buzz start times, end times and durations, we defined the buzz as the time period during which click rate exceeded 125 clicks per second [about three to four times the mean pre-buzz click rate, and slightly higher than the upper values observed in transient variations about that mean (Fig. 2)]. For the purposes of these calculations, a buzz started when the threshold click rate of 125 clicks per second was first exceeded, and ended when the click rate fell below threshold for the last time. Using the above criteria, we calculated the start time, end time and duration of each prey capture buzz, as well as the mean start time, end time and buzz duration for the set of all 67 successful captures. We excluded buzzes that ended more than 5 s before prey capture or began more than 5 s after prey capture in our analysis. As seen in Fig. 2, buzzes outside those time limits did not seem to be associated with prey capture. Rather, the rare buzzes that occurred more than 5 s before capture were probably related to non-prey objects (including landmarks or other porpoises) in the pool, and the buzzes that occurred more than 5 s after capture were probably related to the porpoises' returning to station with the trainers. To assess the effects of eyecups, prey type, and individual porpoise on buzz duration, we log-transformed the buzz duration data to meet normality and homoscedasticity assumptions and then carried out a three-way ANOVA.

Bats and toothed whales often fall silent for a short period following an echolocation buzz; this pause duration (if any) was calculated for each of the 67 successful prey captures by determining the longest inter-click interval in the 5 s following prey capture.

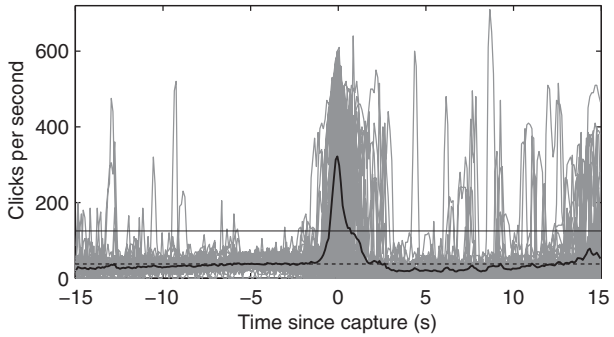

Fig. 2. Click rate as a function of time since prey capture. Each trace is data from one prey capture trial; the thick black line is the mean click rate over all 67 trials. Data are in 0.1 s bins. The dotted black horizontal line indicates the overall mean click rate outside buzzes (37.6 clicks per second), and the thin black horizontal line indicates the threshold used to determine buzz start and end times (125 clicks per second).

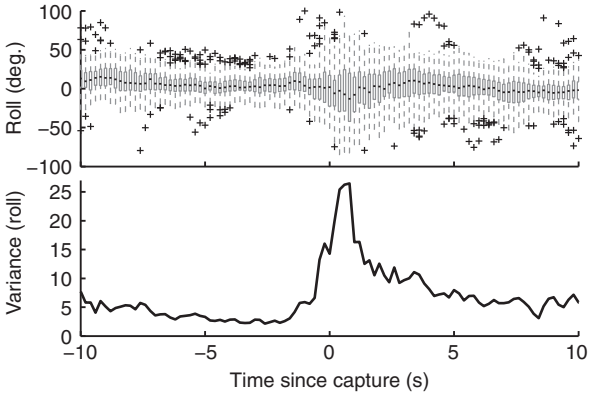

Fig. 3. Roll as a function of time since prey capture. Top panel: box-and-whiskers plot of roll as a function of time for the 67 successful prey captures (data in 0.2 s bins). The black horizontal lines show the median value in each time bin; the top and bottom of the grey rectangles are the upper and lower quartiles within the bin. The dotted grey lines extend to the largest and smallest observed values in the time bin, up to 1.5 times the interquartile range beyond the grey box. Larger and smaller observed values are plotted as black crosses. Bottom panel: variance in roll, calculated for all 67 roll measurements at each sampled time point (sampling rate 5 Hz).

RESULTS

Timing of prey capture

It took the porpoises an average of 19.6 s to find and collect a fish while wearing eyecups, longer than the 15.9 s average time without eyecups; the difference was significant at the P=0.05 level (t-test, d.f.=32, P=0.000027).

Porpoise movements during prey capture

Fig. 3 summarizes the porpoise orientation data. Variability in porpoise roll angle increased around the time of prey capture, indicating that the porpoises turned their bodies more, or more frequently, as they neared the fish and captured it. However, average roll remained relatively constant throughout the trials, indicating that the porpoises did not have a preferred roll angle during their final approach to their prey. They never rolled completely upside down during the prey capture experiments.

Porpoise acoustic behaviour during prey capture

The porpoises produced echolocation buzzes in 66 of the 67 successful prey capture trials. Figs 2 and 4 show the data on click rate as a function of time for all 67 prey capture trials; they clearly indicate that, on average, the porpoises began buzzing before they captured the fish, and continued to buzz after the capture event. The click rate within the buzz generally increased rapidly and peaked around the time of prey capture, with maximum observed buzz click rates averaging 321 clicks per second (3.1 ms ICI) and as high as 640 clicks per second (1.6 ms ICI).

For the 66 captures in which buzzes were detected, the mean buzz start time was 0.53 s before prey capture, end time was 0.83 s after prey capture, and mean buzz duration was 1.37 s. After buzzes, porpoises sometimes paused their production of echolocation clicks, but few post-buzz pauses were long enough to clearly distinguish them from longer ICIs that regularly occurred before the buzz (mean maximum post-buzz ICI 481 ms; pause duration ≥1 s in 9 of 67 trials).

During buzzes, porpoises not only increased their click rate, but also apparently decreased the level of their emitted clicks by about 10 dB compared with the average level outside buzzes. Fig. 5 shows the data on tag-recorded click level as a function of time for all 67 successful prey captures. Because the tag was physically attached to the animal and positioned off-axis, behind the sound generator, these levels are not source levels. They are probably at least 40 dB lower than on-axis source levels (Hansen, 2007). However, the tag-received levels are probably correlated with the source levels (Madsen et al., 2005; Madsen et al., 2002a).

Figs 6–8 compare click rates and levels between varying sets of conditions: with and without eyecups (Fig. 6); Eigil *versus* Sif (Fig. 7); and herring *versus* capelin (Fig. 8). As shown in Fig. 6, the presence or absence of eyecups had no obvious effect on maximum buzz click rate; buzzes appeared to begin slightly earlier in trials with eyecups and to include a second peak in click rate after capture in trials with eyecups, but there was no significant effect of eyecups on buzz duration [three-way ANOVA, F(1 d.f.)=0.43, P=0.50]. Compared with trials without eyecups, click levels during trials with eyecups tended to be a bit lower before capture and a bit higher after. Fig. 7 shows that Sif tended to use click levels about 5–10 dB higher than Eigil in all trials; in addition, her buzz click rate was much faster than his. Sif's buzzes were longer than Eigil's [three-way ANOVA, F(1 d.f.)=11.54, P=0.0012]. Fig. 8 compares click rates and sound levels during trials with herring and capelin.

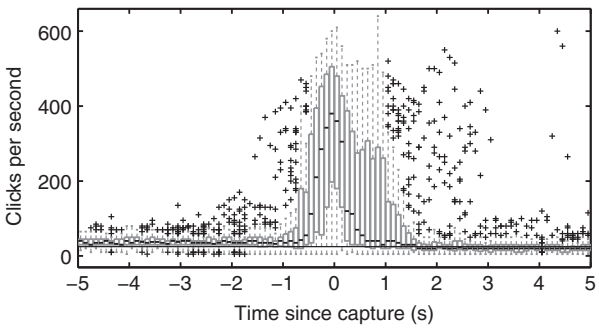

Fig. 4. Box-and-whiskers plot of click rate as a function of time for 67 prey captures by harbour porpoises (data in 0.1 s bins). Symbols and notation are the same as in Fig. 3 (top panel). The black horizontal line indicates median click rate outside buzzes (25 clicks per second). Mean buzz start time was 0.53 s before prey capture, end time was 0.83 s after prey capture, and mean buzz duration was 1.37 s.

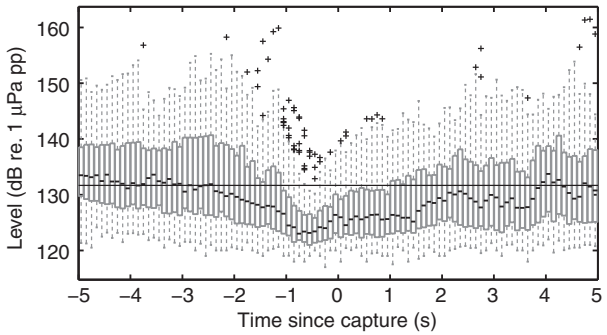

Fig. 5. Box-and-whiskers plot of click level as a function of time for 67 prey captures by harbour porpoises (data in 0.1 s bins). Levels are the off-axis, on-animal levels from the tag recordings, not click source levels. Symbols and notation are the same as in Fig. 3 (top panel). The black horizontal line indicates the median click level outside buzzes (132 dB). Mean buzz start time was 0.53 s before prey capture, end time was 0.83 s after prey capture, and mean buzz duration was 1.37 s.

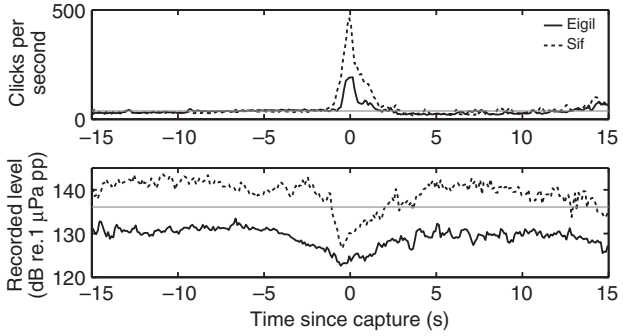

Fig. 7. Porpoise click rates (top panel) and levels (bottom panel) as a function of time. Solid traces show data from trials with Eigil (*N*=33); dotted traces show data from trials with Sif (*N*=34). Data are in 0.1 s bins. Grey horizontal lines indicate the overall mean click rate (37.6 clicks per second) and level (136 dB) outside buzzes.

Although click rates were very similar for the two prey types, the mean click levels were about 3 dB higher for capelin captures, except immediately preceding prey capture, when they were equal. Buzzes were longer during trials with herring than during trials with capelin and sprat [three-way ANOVA, $F(1\,\text{d.f.})=5.06$, $P=0.028$].

In addition to considering variations in click rate and level as functions of time since prey capture, we also investigated recorded click level as a function of inter-click interval, or ICI (Fig. 9). Click levels were relatively constant for ICIs greater than about 40 ms, but they decreased with decreasing ICI for ICIs less than about 40 ms. Fig. 9B shows the click level *versus* ICI data as a scatter plot. The figure does not provide evidence for a clear distinction between buzz clicks and regular clicks on the basis of either ICI or click level. It is important to note that we cannot be completely certain that none of the detected clicks were produced by other animals; some of the clicks in Fig. 9 (perhaps especially the highest-amplitude clicks) may have been produced by animals other than the tagged porpoise.

DISCUSSION

Buzzes

In all 67 of the successful prey capture trials, porpoises produced echolocation clicks throughout the prey capture trial regardless of whether or not they were wearing eyecups; in only one of the 67 trials did the porpoise capture the fish without producing an echolocation buzz [in one trial, Eigil (with eyecups) caught a herring without producing a discernible buzz]. These data and data from the field (Akamatsu et al., 2007) support the notion that porpoises emit echolocation clicks most of the time, and that echolocation is a primary sensory modality for prey localization. The consistent use of buzzes in the present study also indicates that they are an integral part of the capture phase of biosonar-based foraging, for porpoises as for many bats (Schnitzler and Kalko, 2001; Thomas et al., 2004) and larger toothed whales (Johnson et al., 2004; Madsen et al., 2002b; Miller et al., 1995; Miller et al., 2004; Thomas et al., 2004).

On average, the porpoises initiated echolocation buzzes less than a second before prey capture, when they were within about a porpoise body length of the prey fish. Maximum buzz rates exceeded 300 clicks per second on average, and ranged up to 640 clicks per second; highest rates often coincided with the time of prey capture. These buzz click rates are similar to those previously reported for harbour porpoises (several hundred to about 700 clicks per second) (Akamatsu et al., 2007; Verboom and Kastelein, 2004; Verfuss et al., 2009). However, we consider them to be minimum estimates of the actual observed click rates, since we may have failed to detect very low-level buzz clicks (see Click levels section). The minimum ICI during buzzes (on

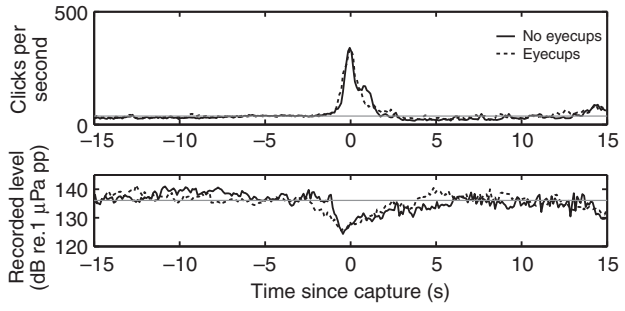

Fig. 6. Porpoise click rates (top panel) and levels (bottom panel) as a function of time. Solid traces show data from trials without eyecups (*N*=34); dotted traces show data from trials with eyecups (*N*=33). Data are in 0.1 s bins. Grey horizontal lines indicate the overall mean click rate (37.6 clicks per second) and level (136 dB) outside buzzes.

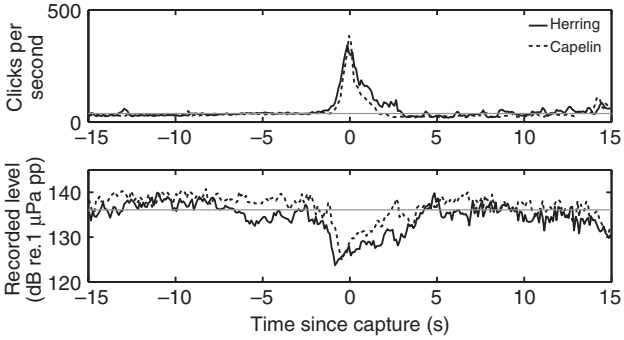

Fig. 8. Porpoise click rates (top panel) and levels (bottom panel) as a function of time. Solid traces show data from trials with herring (*N*=27); dotted traces show data from trials with capelin (*N*=35). Data are in 0.1 s bins. Grey horizontal lines indicate the overall mean click rate (37.6 clicks per second) and level (136 dB) outside buzzes.

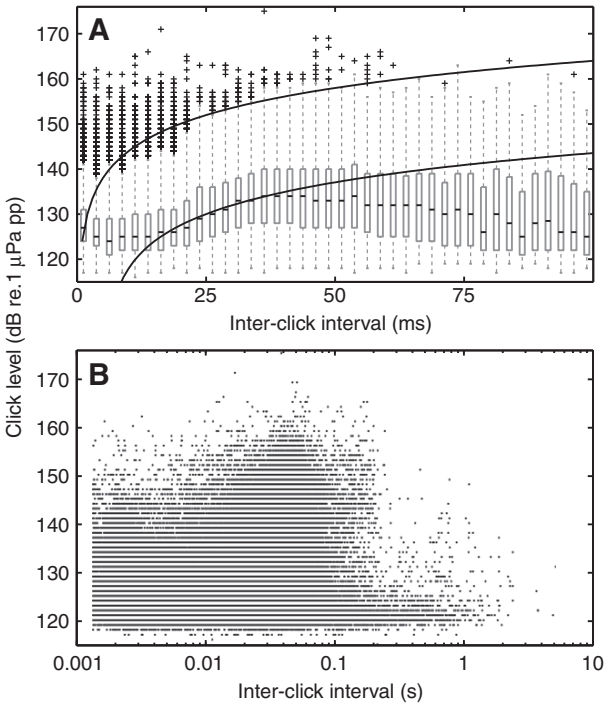

Fig. 9. (A) Box-and-whiskers plot of click level as a function of inter-click interval (ICI). Data are in 2.5 ms bins. Symbols and notation are the same as in Fig. 3 (top panel). The solid black lines show sample $20\log_{10}$(ICI) relationships for comparison with the data. (B) Scatter plot of click levels as a function of ICI.

average 3.1 ms) was much shorter than the auditory processing time estimated for single echoes [20–35 ms (Au et al., 1999)]. Assuming the accuracy of that estimate, our data confirm that although porpoises may adjust their ICI to allow for echo processing time during search and approach phases, they switch to another mode in the terminal phase, termed a 'pitch processing mode' (Verfuss et al., 2009), in which they either process buzz clicks more rapidly or integrate echo information from multiple clicks.

The porpoises studied here manoeuvred more during prey capture than at other times, as indicated by increased variability in roll angle (Fig. 3). Increased variability in body orientation simultaneous with an echolocation buzz may thus be an indicator of prey capture attempts in toothed whales, as suggested by Miller and colleagues for sperm whales (Miller et al., 2004). However, in contrast to sperm whales (Miller et al., 2004) and to porpoises in a previous study conducted at the same facility (Verfuss et al., 2009), the porpoises never rolled upside down during our trials (Fig. 3). These differences could be explained by the fact that we used dead fish rather than live prey, or could signify a change in the animals' behaviour over years in captivity.

Unlike bats, for which the end of the echolocation buzz occurs before or coincides with prey capture (Griffin et al., 1960; Hartley, 1992; Hiryu et al., 2007; Kalko, 1995; Kalko and Schnitzler, 1989; Melcón et al., 2007; Moss and Surlykke, 2001), the harbour porpoises in this study continued their buzzes after prey capture (that is, beyond the start of prey handling). Although porpoises and odontocetes in general are thought to be suction feeders (Kastelein et al., 1997; Werth, 2006), and the porpoises we studied did appear to use suction to get prey into their mouths, we also observed them to manipulate or carry the prey in their mouths for periods of up to a few seconds, generally buzzing throughout this handling time (Fig. 1). A similar extension of the buzz phase may be more difficult for bats that emit sounds through the mouth once they have actually begun to consume prey, since eating prey could interfere with vocalizing. By contrast, the toothed whale sound production system is completely separated from the digestive tract, so prey in the mouth should not interfere with the sound generator. In porpoises, the continuation of the buzz post-capture might also stem from some physiological limitation, but that explanation seems somewhat less likely, considering the extent to which toothed whales can control the timing and spectra of their clicks (Au, 1993). Alternatively, continuing to buzz after capture may allow immediate re-localization of prey items that escape after nearly successful capture attempts or facilitate post-capture pursuit of other, nearby prey items (especially for schooling prey like herring). Finally, we cannot fully exclude the possibility that the extended buzzes we observed have developed over years in captivity, being fed dead fish.

Almost all of the porpoises' prey capture attempts were successful during our experimental trials, which is not surprising considering that we used dead prey items. Consequently, the dataset is not suitable for comparing the post-buzz pause durations and click characteristics of successful and unsuccessful capture attempts.

Click rates

During the approach phase, the average click rate of the porpoises in this study was about 35 clicks per second, corresponding to an ICI of about 29 ms (Figs 2 and 4), which is similar to the minimum ICI (30 ms) observed in a study of free-ranging harbour porpoises in Danish waters (Villadsgaard et al., 2007). The observed ICIs were somewhat less than those observed in a study of the same animals by Verfuss et al. (Verfuss et al., 2009), which might be explained by the fact that the experimental pool was larger at the time of Verfuss' experiments. The mean ICI was relatively constant over time, decreasing slightly from about 39 ms 15 s before capture to about 26 ms just before initiation of the echolocation buzz (Fig. 2), which could be interpreted as a response to reduction in porpoise–prey range. However, the trend is weaker in the median data (Fig. 4). Figs 1, 2 and 4 also show that there was some variability in ICI over the course of individual captures, which often showed bursts of fast clicks followed by resumption of a slower click rate, rather than a consistent reduction in ICI as range decreased leading up to the time of prey capture. It is possible that the porpoises investigated multiple targets during each trial, and were not focusing on detecting the fish the entire time. Previous studies with porpoises provide conflicting findings on this topic, with some results suggesting no significant ICI/range adjustment during foraging (Verfuss et al., 2009) and target detection (Teilmann et al., 2002) tasks and others finding such a relationship during navigation (Verfuss et al., 2005) or presumed foraging activity (Akamatsu et al., 2007; Akamatsu et al., 2005). Although not conclusive, our results are consistent with the idea that porpoise inter-click intervals remain relatively constant as porpoise–prey range declines, then decrease rapidly following buzz initiation. This pattern would match more closely with observations from free-ranging echolocating beaked whales and sperm whales (Madsen et al., 2005). Overall, it seems that the non-buzz ICIs of echolocating toothed whales in general, and also porpoises, are longer than the two-way travel time, but that adjustments in the ICIs are not only, or not necessarily, dictated by the changing two-way travel time to the prey during the initial approach phase.

Click levels

Our results show that porpoises reduce the apparent output of their clicks by about 10 dB during buzzes. Although this observation matches the general trend observed in other toothed whales when they are foraging in the wild, other species display even greater reductions in click levels during buzzes: 15–20 dB for Blainville's beaked whales (Madsen et al., 2005) and about 20 dB for sperm whales (Madsen et al., 2002b). Porpoise average click levels decreased leading up to buzz initiation (Fig. 5), but such a steady decline was not consistently apparent in individual-trial data (Fig. 1). Our data also indicate that apparent click levels decrease as click rates increase; unlike beaked whales (Madsen et al., 2005), for porpoises there is no clear separation between regular and buzz clicks in the level/ICI plane (Fig. 9), at least when recorded off the acoustic axis. This result may indicate that porpoises purposefully reduce the source level of faster clicks, perhaps to reduce clutter echoes and focus on a single target, or to maximize their ability to detect returning echoes at close ranges (Supin et al., 2005; Supin et al., 2007; Supin et al., 2008). It is also possible that the porpoise click generator is restricted in the acoustic energy it can produce per unit time, resulting in lower click levels at higher click rates, as observed by Beedholm and Miller (Beedholm and Miller, 2007). Transmit-side automatic gain control (AGC), in which transmission power varies as a function of source–target range to adjust for transmission loss and to stabilise echo levels (Au and Benoit-Bird, 2003), could also result in an ICI/level relationship if ICI is proportional to range (r). In previous work with some of the same animals we studied, click level varied according to $14–17\log_{10}(r)$ or $\log_{10}(ICI)$ (Beedholm and Miller, 2007) or $20\log_{10}(r)$ (Atem et al., 2009) as porpoises approached real or simulated targets in a limited number of trials. An apparent level increase of about 6 dB per doubling of ICI [$20\log_{10}(ICI)$] does not provide a clear fit to our data (Fig. 9), as click levels were highly variable both within and between trials (Figs 1 and 5). Our data thus suggest that any range/time varying output adjustments are not mechanically hardwired to target range through a strong ICI to two-way travel time adjustment, as also demonstrated recently for bottlenose dolphins (Jensen et al., 2009).

The lowest click level detectable in the tag recordings was 117 dB re. 1 μPa (peak-to-peak; pp). Because of the position of the tag on the animal, on-tag click levels are probably ~40 dB lower than on-axis source levels (Hansen, 2007). Although our tag threshold was much lower than the detection threshold (136 dB re. 1 μPa pp) of tags previously deployed on porpoises in a similar position (Akamatsu et al., 2007), we were still not able to detect every click, especially low-level buzz clicks. Since lower-level clicks tended to occur near the start or end of buzzes, these detection limitations could have led us to underestimate level reductions during buzzes or introduced some error into our estimates of buzz start and/or end times.

Effects of eyecups, individual, and prey type

There were no major differences in echolocation phases or click rates and levels between our trials with and without eyecups. However, porpoises took longer to capture prey with eyecups, so visual input, when available, seems to facilitate prey capture in some way.

We observed a striking difference in click levels between the two animals that participated in the study; Sif's clicks had about 5–10 dB higher amplitude on the tag than Eigil's, and her buzz click rates were faster than Eigil's (possibly because of level and/or detectability differences). Small but statistically significant differences in average click source levels have previously been reported for these animals (Atem et al., 2009). Sif is thought to have sustained minor hearing damage in the past that has caused her to increase her outgoing echolocation click levels (M.W., unpublished observation), so the differences between Sif and Eigil may exceed the normal range of intraspecific variation. Nevertheless, they provide a benchmark for the click level variations that may result from differences in hearing sensitivity, and emphasize the need to include more animals in audiology and biosonar experiments.

Interestingly, we also observed differences in click levels between trials with herring and capelin; apparent click amplitudes were about 3 dB higher for capelin than for herring (Fig. 7). Many bats employ AGC to compensate for transmission loss (Hartley, 1992; Surlykke and Kalko, 2008), but changes in source level to compensate for variations in prey target strength have not previously been reported [but see Au (Au, 1993) for a brief discussion of the topic for dolphins]. The average acoustic target strength of the capelin used in our experiments was measured to be –55 dB, about 18 dB less than that of the herring (–37 dB; S.D., unpublished observation). Since the difference in target strengths so exceeds the apparent increase in click amplitude, it seems clear that the porpoises were not using source-level adjustment alone to keep echo levels from the two prey types constant. Our findings are consistent with data on bats collected by Boonman and Jones (Boonman and Jones, 2002), who observed a 4 dB increase in source level when target strength was reduced by 17–18 dB, a change they judged insignificant. However, the mismatch between target strength and level increase does not automatically imply this conclusion. It is possible that acoustic clutter could have limited maximum source levels used by the animals in their pen. Alternately, animals may adjust their source levels to maintain target detectability rather than to stabilize echo levels (Au, 1993), for which a modest 3 dB increase in outgoing click level could have been sufficient. Finally, perceived echo intensity is determined not only by click levels and target strength, but also by transmission loss and auditory sensitivity (which may vary by situation, including possible forward masking by the outgoing click) (Supin et al., 2005; Supin et al., 2007; Supin et al., 2008).

Conclusions

Echolocating harbour porpoises used relatively stable mean click intervals (mean 29 ms) during search and initial approach phases. A decrease in ICI from about 39 to 26 ms over the course of approach was evident in the data average but less so in individual trial data, which showed significant click-to-click variability and few linear trends. When ~1–2 porpoise body lengths away from the fish, the porpoises initiated an echolocation buzz, during which inter-click intervals decreased by an order of magnitude, and apparent source levels decreased by about 10 dB. The most striking finding of this study is that the porpoises continued to buzz after they had reached prey and begun to handle it in their mouths. They generally intercepted prey about halfway into the buzz during increased manoeuvring, which illustrates that buzz termination does not necessarily correspond to the moment of prey capture, and suggests that buzzes may have functions other than providing detailed information on target location leading up to capture. These functions remain unknown, and could include re-capturing escaping prey, or closely monitoring the acoustic scene immediately surrounding the porpoise for other prey, landmarks or objects of interest. The echolocation behaviour of the porpoises in this study – slow clicking during search and approach and buzzing during prey capture

– is akin to that of other much larger toothed whales, but the porpoises seem to operate a shorter range biosonar system, with faster overall click rates during search, approach and interception of prey.

LIST OF ABBREVIATIONS

AGC	automatic gain control
dB	decibels (dB)
ICI	inter-click interval
pp	peak-to-peak
r	range

We are very grateful to Ida Eskessen, Sanja Heikillä, Lara Delgado, Michael Hansen, Anne Villadsgaard, Kristian Beedholm, Lee Miller, and everyone else at the Fjord & Baelt Center for help with data collection, and helpful advice. We also thank Tom Hurst, Mark Johnson, Alex Bocconcelli and Jeremy Winn, who provided Dtag materials, as well as help with tag design and construction. Carrick Detweiler and Iuliu Vasilescu assisted with suction cup fabrication. This project was funded by grant 32031300 from the WHOI Ocean Life Institute. All experiments with porpoises were approved by the WHOI Institutional Animal Care and Use Committee. The animals are maintained by Fjord & Bælt, Kerteminde, Denmark, under permits no. SN 343/FY-0014 and 1996-3446-0021 from the Danish Forest and Nature Agency, Danish Ministry of Environment.

REFERENCES

Aguilar Soto, N., Johnson, M. P., Madsen, P. T., Díaz, F., Domínguez, I., Brito, A. and Tyack, P. L. (2008). Cheetahs of the deep sea: deep foraging sprints in short-finned pilot whales off Tenerife (Canary Islands). *J. Anim. Ecol.* **77**, 936-947.

Akamatsu, T., Wang, D., Wang, K. X. and Naito, Y. (2005). Biosonar behaviour of free-ranging porpoises. *Proc. Biol. Sci.* **272**, 797-801.

Akamatsu, T., Teilmann, J., Miller, L. A., Tougaard, J., Dietz, R., Wang, D., Wang, K. X., Siebert, U. and Naito, Y. (2007). Comparison of echolocation behaviour between coastal and riverine porpoises. *Deep-Sea Res. Part II Top. Stud. Oceanogr.* **54**, 290-297.

Atem, A. C. G., Rasmussen, M. H., Wahlberg, M., Petersen, H. C. and Miller, L. A. (2009). Changes in click source levels with distance to targets: Studies of free-ranging white-beaked dolphins (*Lagenorhynchus albirostris*) and captive harbor porpoises (*Phocoena phocoena*). *Bioacoustics* **19** (in press).

Au, W. W. L. (1993). *The Sonar of Dolphins*. New York: Springer-Verlag.

Au, W. W. L. and Benoit-Bird, K. J. (2003). Automatic gain control in the echolocation system of dolphins. *Nature* **423**, 861-863.

Au, W. W. L., Kastelein, R. A., Rippe, T. and Schooneman, N. M. (1999). Transmission beam pattern and echolocation signals of a harbor porpoise (*Phocoena phocoena*). *J. Acoust. Soc. Am.* **106**, 3699-3705.

Beedholm, K. and Miller, L. A. (2007). Automatic gain control in harbor porpoises (*Phocoena phocoena*)? Central versus peripheral mechanisms. *Aquat. Mamm.* **33**, 69-75.

Boonman, A. and Jones, G. (2002). Intensity control during target approach in echolocating bats; stereotypical sensori-motor behaviour in Daubenton's bats, *Myotis daubentonii*. *J. Exp. Biol.* **205**, 2865-2874.

Britton, A. R. C. and Jones, G. (1999). Echolocation behaviour and prey-capture success in foraging bats: laboratory and field experiments on *Myotis daubentonii*. *J. Exp. Biol.* **202**, 1793-1801.

DeRuiter, S. L. (2008). *Echolocation-based Foraging by Harbor Porpoises and Sperm Whales, Including Effects of Noise Exposure and Sound Propagation*. PhD thesis, Massachusetts Institute of Technology/Woods Hole Oceanographic Institution Joint Program, Cambridge and Woods Hole, MA.

Evans, W. E. (1973). Echolocation by marine delphinids and one species of freshwater dolphin. *J. Acoust. Soc. Am.* **54**, 191-199.

Griffin, D. R. (1958). *Listening in the Dark*. New Haven, CT: Yale University Press.

Griffin, D. R., Webster, F. A. and Michael, C. R. (1960). The echolocation of flying insects by bats. *Anim. Behav.* **8**, 141-154.

Hansen, M. (2007). *High and Low Frequency Components in Harbour Porpoise (Phocoena phocoena) Clicks for Echolocation and Communication - Facts or Artefacts*? MSc Thesis, University of Aarhus, Aarhus, Denmark.

Hartley, D. J. (1992). Stabilization of perceived echo amplitudes in echolocating bats. 2. The acoustic behavior of the big brown bat, *Eptesicus fuscus*, when tracking moving prey. *J. Acoust. Soc. Am.* **91**, 1133-1149.

Hiryu, S., Hagino, T., Riquimaroux, H. and Watanabe, Y. (2007). Echo-intensity compensation in echolocating bats (*Pipistrellus abramus*) during flight measured by a telemetry microphone. *J. Acoust. Soc. Am.* **121**, 1749-1757.

Jensen, F. H., Bejder, L., Wahlberg, M. and Madsen, P. T. (2009). Biosonar adjustments to target range of echolocating bottlenose dolphins (*Tursiops* sp.) in the wild. *J. Exp. Biol.* **212**, 1078-1086.

Johnson, M., Madsen, P. T., Zimmer, W. M. X., de Soto, N. A. and Tyack, P. L. (2006). Foraging Blainville's beaked whales (*Mesoplodon densirostris*) produce distinct click types matched to different phases of echolocation. *J. Exp. Biol.* **209**, 5038-5050.

Johnson, M., Hickmott, L. S., Soto, N. A. and Madsen, P. T. (2008). Echolocation behaviour adapted to prey in foraging Blainville's beaked whale (*Mesoplodon densirostris*). *Proc. Biol. Sci.* **275**, 133-139.

Johnson, M. P. and Tyack, P. L. (2003). A digital acoustic recording tag for measuring the response of wild marine mammals to sound. *IEEE J. Oceanic Eng.* **28**, 3-12.

Johnson, M. P., Madsen, P. T., Zimmer, W. M. X., de Soto, N. A. and Tyack, P. L. (2004). Beaked whales echolocate on prey. *Biol. Lett.* **271**, S383-S386.

Kalko, E. K. V. (1995). Insect pursuit, prey capture and echolocation in pipistrelle bats (Microchiroptera). *Anim. Behav.* **50**, 861-880.

Kalko, E. K. V. and Schnitzler, H. U. (1989). The echolocation and hunting behavior of daubenton bat, *Myotis daubentoni*. *Behav. Ecol. Sociobiol.* **24**, 225-238.

Kastelein, R. A., Staal, C., Terlouw, A. and Muller, M. (1997). Pressure changes in the mouth of a feeding harbour porpoise (*Phocoena phocoena*). In *The Biology of The Harbor Porpoise* (ed. A. J. Read, P. R. Wiepkma and P. E. Nachtigall), pp. 279-291. Woerden, The Netherlands: De Spil Publishers.

Lockyer, C. (2003). Harbour porpoises (*Phocoena phocoena*) in the North Atlantic: biological parameters. In *Harbour Porpoises in the North Atlantic*, vol. 5 (ed. T. Haug, G. Desportes, G. A. Vikingsson and L. Witting), pp. 71-89. Tromsø, Norway: North Atlantic Marine Mammal Commission Scientific Publications.

Madsen, P. T., Payne, R., Kristiansen, N. U., Wahlberg, M., Kerr, I. and Møhl, B. (2002a). Sperm whale sound production studied with ultrasound time/depth recording tags. *J. Exp. Biol.* **205**, 1899-1906.

Madsen, P. T., Wahlberg, M. and Møhl, B. (2002b). Male sperm whale (*Physeter macrocephalus*) acoustics in a high-latitude habitat: implications for echolocation and communication. *Behav. Ecol. Sociobiol.* **53**, 31-41.

Madsen, P. T., Johnson, M., de Soto, N. A., Zimmer, W. M. X. and Tyack, P. (2005). Biosonar performance of foraging beaked whales (*Mesoplodon densirostris*). *J. Exp. Biol.* **208**, 181-194.

Melcón, M. L., Denzinger, A. and Schnitzler, H. U. (2007). Aerial hawking and landing: approach behaviour in Natterer's bats, *Myotis nattereri* (Kuhl 1818). *J. Exp. Biol.* **210**, 4457-4464.

Miller, L. A., Pristed, J., Møhl, B. and Surlykke, A. (1995). The click-sounds of narwhals (*Monodon monoceros*) in Inglefield Bay, Northwest Greenland. *Mar. Mamm. Sci.* **11**, 491-502.

Miller, P. J., Johnson, M. P. and Tyack, P. L. (2004). Sperm whale behavior indicates the use of echolocation click buzzes 'creaks' in prey capture. *Proc. Biol. Sci.* **271**, 2239-2247.

Møhl, B., Wahlberg, M., Madsen, P. T., Heerfordt, A. and Lund, A. (2003). The monopulsed nature of sperm whale clicks. *J. Acoust. Soc. Am.* **114**, 1143-1154.

Moss, C. F. and Surlykke, A. (2001). Auditory scene analysis by echolocation in bats. *J. Acoust. Soc. Am.* **110**, 2207-2226.

Ramirez, K. (1999). *Animal Training: Successful Animal Management Through Positive Reinforcement*. Chicago, IL: Shedd Aquarium Society.

Reynolds, J. E. I. and Rommel, S. A. (1999). *Biology of Marine Mammals*. Washington, DC: Smithsonian Institution Press.

Schnitzler, H. U. and Kalko, E. K. V. (2001). Echolocation by insect-eating bats. *Bioscience* **51**, 557-569.

Supin, A. Y., Nachtigall, P. E., Au, W. W. L. and Breese, M. (2005). Invariance of evoked-potential echo-responses to target strength and distance in an echolocating false killer whale. *J. Acoust. Soc. Am.* **117**, 3928-3935.

Supin, A. Y., Nachtigall, P. E. and Breese, M. (2007). Evoked-potential recovery during double click stimulation in a whale: a possibility of biosonar automatic gain control. *J. Acoust. Soc. Am.* **121**, 618-625.

Supin, A. Y., Nachtigall, P. E. and Breese, M. (2008). Hearing sensitivity during target presence and absence while a whale echolocates. *J. Acoust. Soc. Am.* **123**, 534-541.

Surlykke, A. and Kalko, E. K. (2008). Echolocating bats cry out loud to detect their prey. *PLoS ONE* **3**, e2036.

Teilmann, J., Miller, L. A., Kirketerp, T., Kastelein, R. A., Madsen, P. T., Neilsen, B. K. and Au, W. W. L. (2002). Characteristics of echolocation signals used by a harbour porpoise (*Phocoena phocoena*) in a target detection experiment. *Aquat. Mamm.* **28**, 275-284.

Teloni, V., Johnson, M. P., Miller, P. J. O. and Madsen, P. T. (2008). Shallow food for deep divers: dynamic foraging behavior of male sperm whales in a high latitude habitat. *J. Exp. Mar. Biol. Ecol.* **354**, 119-131.

Thomas, J. A., Moss, C. F. and Vater, M. (2004). *Echolocation in Bats and Dolphins*. Chicago, IL: University of Chicago Press.

Tyack, P. L., Johnson, M., Soto, N. A., Sturlese, A. and Madsen, P. T. (2006). Extreme diving of beaked whales. *J. Exp. Biol.* **209**, 4238-4253.

Verboom, W. C. and Kastelein, R. A. (2004). Structure of harbor porpoise (*Phocoena phocoena*) acoustic signals with high repetition rates. In *Echolocation in Bats and Dolphins* (ed. J. A. Thomas, C. F. Moss and M. Vater), pp. 40-43. Chicago, IL: University of Chicago Press.

Verfuss, U. K., Miller, L. A. and Schnitzler, H. U. (2005). Spatial orientation in echolocating harbour porpoises (*Phocoena phocoena*). *J. Exp. Biol.* **208**, 3385-3394.

Verfuss, U. K., Miller, L. A., Pilz, P. K. D. and Schnitzler, H. U. (2009). Echolocation by two foraging harbor porpoises. *J. Exp. Biol.* **212**, 823-834.

Villadsgaard, A., Wahlberg, M. and Tougaard, J. (2007). Echolocation signals of wild harbour porpoises, *Phocoena phocoena*. *J. Exp. Biol.* **210**, 56-64.

Watwood, S. L., Miller, P. J. O., Johnson, M., Madsen, P. T. and Tyack, P. L. (2006). Deep-diving foraging behaviour of sperm whales (*Physeter macrocephalus*). *J. Anim. Ecol.* **75**, 814-825.

Werth, A. J. (2006). Odontocete suction feeding: experimental analysis of water flow and head shape. *J. Morphol.* **267**, 1415-1428.